WEAR ANALYSIS OF HOT FORGING DIES


A THESIS SUBMITTED TO
THE GRADUATE SCHOOL OF NATURAL AND APPLIED SCIENCES
OF
THE MIDDLE EAST TECHNICAL UNIVERSITY


BY


SIAMAK ABACHI


IN PARTIAL FULFILLMENT OF THE REQUIREMENTS
FOR THE DEGREE OF MASTER OF SCIENCE

IN

THE DEPARTMENT OF MECHANICAL ENGINEERING


DECEMBER 2004

Approval of the Graduate School of Natural and Applied Sciences.

_____

Prof. Dr. Canan ÖZGEN
Director

I certify that this thesis satisfies all the requirements as a thesis for the degree of Master of Science.

_____

Prof. Dr. Kemal İDER
Head of the Department

This is to certify that we have read this thesis and that in our opinion it is fully adequate, in scope and quality, as a thesis for the degree of Master of Science.

_____     _____

Prof. Dr. Mustafa İlhan GÖKLER        Prof. Dr. Metin AKKÖK
Co-Supervisor                    Supervisor

Examining Committee Members:

Prof. Dr. R. Orhan YILDIRIM       _____

Prof. Dr. Metin AKKÖK            _____

Prof. Dr. Mustafa İlhan GÖKLER    _____

Prof. Dr. Haluk DARENDELİLER    _____

Prof. Dr. Bilgehan ÖGEL           _____

I hereby declare that all information in this document has been obtained and presented in accordance with academic rules and ethical conduct. I also declare that, as required by these rules and conduct, I have fully cited and referenced all material and results that are not original to this work.

Name, Last name :  Siamak ABACHI

Signature           :

# ABSTRACT


# WEAR ANALYSIS OF HOT FORGING DIES


**ABACHI, Siamak**


**M. S., Department of Mechanical Engineering**
**Supervisor: Prof. Dr. Metin AKKÖK**
**Co-Supervisor: Prof. Dr. Mustafa İlhan GÖKLER**


**December 2004, 94 pages**


The service lives of dies in forging processes are to a large extent limited by wear, fatigue fracture and plastic deformation, etc. In hot forging processes, wear is the predominant factor in the operating lives of dies. In this study, the wear analysis of a closed die at the final stage of a hot forging process has been realized. The preform geometry of the part to be forged was measured by Coordinate Measuring Machine (CMM), and the CAD model of the die and the worn die were provided by the particular forging company. The hot forging operation was carried out at a workpiece temperature of 1100°C and die temperature of 300°C for a batch of 678 on a 1600-ton mechanical press. The die and the workpiece materials were AISI L6 tool steel and DIN 1.4021, respectively.

The simulation of forging process for the die and the workpiece was carried out by Finite Volume Method using MSC.SuperForge. The flow of the material in the die, die filling, contact pressure distribution, sliding velocities and temperature distribution of the die have been investigated. In a single stroke, the depth of wear was evaluated using Archard's wear equation with a constant wear coefficient of $1\times10^{-12}$ Pa$^{-1}$ as an initial value. The depth of wear

on the die surface in every step has been evaluated using the Finite Volume simulation results and then the total depth of wear was determined. To be able to compare the wear analysis results with the experimental worn die, the surface measurement of the worn die has been done on CMM. By comparing the numerical results of the die wear analysis with the worn die measurement, the dimensional wear coefficient has been evaluated for different points of the die surface and finally a value of dimensional wear coefficient is suggested. As a result, the wear coefficient was evaluated as $6.5 \times 10^{-13}$ $Pa^{-1}$ and considered as a good approximation to obtain the wear depth and the die life in hot forging processes under similar conditions.

**Keywords:** Wear, Wear Model, Wear Coefficient, Metal Forming, Hot Forging, Closed-Die Forging, Finite Volume Analysis.

# ÖZ

## SICAK DÖVME KALIPLARININ AŞINMA ANALİZİ

**ABACHI, Siamak**

**Yüksek Lisans, Makine Mühendisliği Bölümü**
**Tez Yöneticisi: Prof. Dr. Metin AKKÖK**
**Ortak Tez Yöneticisi: Prof. Dr. Mustafa İlhan GÖKLER**

**Aralık 2004, 94 sayfa**

Dövme işleminde kullanılan kalıpların servis ömürleri büyük oranda aşınma, yorulma kırılması ve kalıcı şekil değişimleri gibi nedenlerle sınırlıdır. Sıcak dövme işlemlerinde aşınma, kalıpların servis ömürlerinde en baskın faktördür. Bu çalışmada, bir sıcak dövme işleminin son aşamasında kapalı bir kalıptaki aşınma analizi gerçekleştirilmiştir. Dövülecek parçanın ilk geometrisi koordinat ölçüm cihazı (CMM) ile ölçülmüş ve parçaya ait bilgisayar modeli ve bir kafile üretiminde aşınmış kalıp bir dövme firması tarafından sağlanmıştır. Sıcak dövme işlemi 1100°C sıcaklıktaki iş parçası ve 300°C sıcaklıktaki kalıp ile 1600 tonluk mekanik preste 678 parça üretilerek gerçekleştirilmiştir. Kalıp ve iş parçası sırasıyla AISI L6 takım çeliği ve DIN 1.4021 kod numaralı malzemelerdir.

Kalıp ve iş parçası için dövme işleminin benzetimi Sonlu Hacim Metodu kullanılarak MSC.SuperForge yazılımı ile gerçekleştirilmiştir. Kalıp içerisindeki malzeme akışı, malzemenin kalıp içini dolduruşu, temas basınç dağılımı, kayma hızları, kalıp yüzey ve sıcaklık dağılımı incelenmiştir. Tek bir dövme işlemindeki aşınma miktarı, başlangıç değeri olarak $1\times10^{-12}$ Pa$^{-1}$

sabit aşınma katsayısı ile Archard denklemi kullanılarak elde edilmiştir. Kalıp yüzeyinde aşınma derinliği Sonlu Hacim benzetimi sonuçlarının her adımında tespit edilmiş ve toplam aşınma miktarı belirlenmiştir. Aşınma analizi sonuçlarını, aşınmış kalıp değerleriyle karşılaştırmak için aşınmaya maruz kalan kalıba ait yüzey ölçümleri  CMM cihazı ile yapılmıştır. Kalıp aşınmasına ait sayısal sonuçlarını aşınmış kalıp değerleriyle karşılaştırılmasıyla kalıp yüzeyindeki farklı noktalar için  boyutsal aşınma katsayıları elde edilmiş ve sonunda boyutsal bir aşınma katsayısı önerilmiştir. Sonuç olarak, aşınma katsayısı $6.5 \times 10^{-13}$ $Pa^{-1}$ olarak belirlenmiş ve benzer şartlardaki sıcak dövme işlemlerinde kullanılan  kalıp  ömürlerinin ve aşınma miktarlarının (derinlikleri) belirlenmesi için iyi bir yaklaşım sağladığı görülmüştür.

**Anahtar Kelimeler:** Aşınma, Aşınma Modeli, Aşınma Katsayısı, Metal Şekillendirme, Sıcak Dövme, Kapalı Kalıpta Dövme, Sonlu Hacim Analizi.

**To My Parents**

# ACKNOWLEDGEMENTS

# TABALE OF CONTENTS

# LIST OF TABLES

TABLES

# LIST OF FIGURES

FIGURES

# LIST OF SYMBOLS

SYMBOL

| | |
|---|---|
| $P$ | Normal contact pressure |
| $\tilde{P}$ | Normalized, non-dimensional, pressure |
| $U$ | Relative sliding velocity |
| $\tilde{U}$ | Normalized, non-dimensional, velocity |
| $w$ | Volume of wear in sliding distance |
| $\tilde{w}$ | Normalized, non-dimensional, wear |
| $K$ | Non-dimensional wear coefficient |
| $k$ | Dimensional wear coefficient |
| $K_{adh}$ | Non-dimensional adhesive wear coefficient |
| $K_{abr}$ | Non-dimensional abrasive wear coefficient |
| $H$ | Hardness of the wearing material |
| $a$ | Thermal diffusivity of the wearing material |
| $A_{nom}$ | Nominal contact area |
| $\psi$ | Bulk shear strength |
| $\tau$ | Interfacial shear strength |
| $m$ | Friction factor |
| $\alpha$ | Heat distribution coefficient between bodies |
| $\mu$ | Coefficient of friction |
| $H_0$ | Hardness of steel in steady state condition |
| $L$ | Latent heat of fusion per unit volume for metal |
| $T_m$ | Melting temperature of metal |
| $T_0$ | Sink temperature of bulk heating |
| $T^*$ | An equivalent temperature for metal |

| | |
|---|---|
| $T_{flash}$ | Flash temperature |
| $T_b$ | Bulk temperature of surface |
| $T_m^{ox}$ | Melting point for oxide |
| $\beta$ | Dimensionless parameter for bulk heating |
| $Q_0$ | Activation energy for the static oxidation of iron |
| $R$ | The universal molar gas constant |
| $c$ | Constant used in the model for mild-oxidation wear |
| $f_m$ | Factor which accounts for the proportion of the molten oxide which is  lost from the surface. |
| $K_{ox}$ | Thermal conductivity of oxide |
| $L_{ox}$ | Latent heat of oxide melting |
| $N$ | Number of contacting asperities |
| $F_N$ | Normal load on contact interface |
| $V$ | Volume of worn material |
| $L$ | Sliding length |
| $M$ | Tempering parameter |
| $T_{temper}$ | Tempering temperature |
| $t$ | Tempering time |
| $d$ | Depth of wear |
| $d_{fin}$ | Final depth of wear in a point after $n$ times forging |

# CHAPTER 1

# INTRODUCTION

Among all manufacturing processes, forging technology has a special place because it helps to produce parts of superior mechanical properties with minimum waste of material. In forging, the starting material has a relatively simple geometry; this material is plastically deformed in one or more operations into a product of relatively complex configuration. Forging usually requires relatively expensive tooling. Thus, the process is economically attractive when a large number of parts must be produced and/or when the mechanical properties required in the finished product can be obtained only by a forging process.

The ever-increasing costs of material, energy and especially manpower require that forging processes and tooling be designed and developed with minimum amount of trial and error with shortest possible lead times. Therefore, to remain competitive, the cost-effective application of computer aided techniques, i.e. CAD, CAM, CAE and especially Finite Element Analysis (FEA) and Finite Volume Analysis (FVA) based computer simulation, are an absolute necessity. The practical use of these techniques requires knowledge of the principal variables of the forging process and their interactions. These variables include: a) the flow behavior of the forged material under processing conditions, b) die geometry and materials, c) friction and lubrication, d) the mechanics of deformation, i.e. strains and stresses, e) the characteristics of the forging equipment, f) the geometry, tolerances, surface finish and mechanical properties of the forging, and g) the effects of the process on the environment [1].

1

In forging process the service life of dies is very important due to economical reasons and also finishing quality of productions. The factors influencing die life are thermal fatigue, plastic deformation, wear, etc. Amongst these, wear is the predominating factor in hot forging process. Lange reported that wear is the dominating failure mechanism for forging dies, being responsible for approximately 70% of failures [2].

## 1.1 Forging Process

There are various classifications applied for the forging process. In general, forging processes can be classified as:

- Temperature: Hot Forging, Cold Forging, Warm Forging
- Type of Machine Used: Hammer, Press, Horizontal Upsetting Machine, Roll Forging, etc.
- Type of die set: Closed die, Open die

### 1.1.1 Classification of Forging Process According to Temperature

In hot forging, the billet is heated above its recrystallization temperature thus avoiding strain hardening. A greater degree of deformation can be achieved in a single operation than in cold or warm forging method. Die wear is also reduced in hot forging. However, the requirements for uniform and controllable die heating systems, formation of the scale and low dimensional accuracy are the main disadvantages of this process.

The temperature of metals being cold forged may range from room temperature to several hundred degrees. The primary advantage is the material savings achieved through precision shapes that require little finishing. While cold forging usually improves mechanical properties, the improvement is not useful in many common applications and economic advantages remain the primary interest. Tool design and manufacture are critical.

Warm forging has a number of cost-saving advantages that underscore its increasing use as a manufacturing method. This process is performed with the workpiece heated to a range that is generally above the work hardening

temperature and below the temperature at which scale forms. Such forgings can be manufactured with excellent definition and can incorporate features that are not possible with conventional forgings. Compared with cold forging, warm forging has the potential advantages of: reduced tooling loads, reduced press loads, increased steel ductility, elimination of need to anneal prior to forging, and favorable as-forged properties that can eliminate heat treatment. Shafts, gears and automotive front wheel drive tulips are some examples for warm forged components [3].

### 1.1.2 Classification of Forging Machines

Forgings can be classified into four main categories according to the type of machine used [4]. These are,

- Hammer Forging (Board Drop Hammers, Power Drop Hammers, Air-Lift Gravity Drop Hammers, Counterblow Hammers)
- Press Forging (Mechanical Presses, Hydraulic Presses, Multiple Ram Presses, Friction Screw Presses)
- Horizontal Forging Machine
- Roll Forging

Forgings made by using mechanical press is discussed in this section, since these type of forging machines are the most commonly used forging equipment in industry. The characteristics of these machines have been given in several publications [3, 4 and 5].

With the exception of the counterblow hammer, forging hammers have a weighted ram, which moves vertically in a downward stroke; thus, exerts a striking force against a stationary component of the anvil near the base of the hammer. The upper half of a pair of dies is fastened to the weighted ram, and lower half to the anvil cap. Initially heated billet is placed on the lower die, and the striking force is imposed on the work metal by the upper die and ram, causing it to deform plastically with each successive blow. The hammer is an

energy-restricted machine. During a working stroke, the deformation proceeds until the total kinetic energy is dissipated by plastic deformation of the forging stock and by elastic deformation of the ram and anvil when the die faces contact with each other. Some of the energy is dissipated as heat loss.

Forging presses generally incorporate a ram that moves in a vertical direction to exert a squeezing action on the workpiece. Depending on the source of the power, forging presses are classified as mechanical or hydraulic. The operation of hydraulic press is relatively simple and is based on the motion of a hydraulic piston guided in a cylinder. Hydraulic presses are essentially load- restricted machines. Maximum capacities exceeding those of the largest power drop hammers are developed by hydraulic presses. Since most of the load is available during the entire stroke, relatively large energies are available for deformation. Within the capacity of a hydraulic press, the maximum load can be limited to protect the tooling and within the limits of the machine, the ram speed can be varied continuously during an entire stroke cycle with an adequate control system. In general, presses can produce all types of the forgings that can be produced by hammers and in addition some alloys of moderate ductility that would break under the blows of a hammer can be forged.

The mechanical forging press is an efficient machine, and it is the most widely used equipment for closed-die forging. The drive of the most mechanical presses is based on a slider-crank mechanism that translates rotary motion into reciprocating linear motion. The eccentric shaft is connected through a clutch and brake system directly to the flywheel. For larger capacities, the flywheel is located on the pinion shaft, which drives the eccentric shaft. The constant clutch torque is available at the eccentric shaft, which transmits the torque and the flywheel energy to the slide through the connecting rod. The flywheel, which is driven by an electric motor, stores energy that is used during deformation of the forged part.

There are some advantages and disadvantages of forging presses. The crank and eccentric presses are displacement-restricted machines. The slide velocity and the available slide load vary in accordance with the position of

the slide before the bottom dead center. Higher production rates are possible with presses than with hammers. Because the impact is less in presses than in hammers, the dies can be less massive, thus requiring less tool steel to make the dies.

### 1.1.3  Classification of Die Set

Open die forging is a forming process that uses standard flat, V-shaped, concave or convex dies in presses. Open die forging processes allow the grain flow in one or two directions. The workpiece is generally compressed in the axial direction (direction of the movement of the upper die) with no lateral constraint. Lateral dimensions are developed by controlling the amount of axial deflection, or by rotating the workpiece. In addition to round, square, rectangular, hexagonal bars and other basic shapes, open-die processes can produce step shafts, solid shafts (spindles or rotors) whose diameter increase or decrease (steps down) at multiple locations along the longitudinal axis; hollows cylindrical in shape, usually with length much greater than the diameter of the part (Length, wall thickness, inner and outer diameter can be varied as needed); ring-like parts; contour-formed metal shells like pressure vessels, which may incorporate extruded nozzles and other design features.

Closed die forging (also called as impression die forging) is basically the shaping of metals in between closed die cavities. As the two dies approach, the workpiece undergoes plastic deformation, flowing laterally until it touches the side walls of the impression. Therefore, the dimensional control of the forging in lateral directions is controlled by the walls of the die, and is ensured by complete fill. Dimensional control in the axial direction is achieved by bringing the die faces to a predetermined position [4].

Flash is the metal, which is forced outward from the workpiece while it is being forged to the configuration of the closed-die impression. In other means, it is the metal in excess of that required to fill the impression. The flash that extends beyond the flash land is contained in a holder referred to as the flash gutter. The gutter, an integral part of the dies, is intentionally designed to

some extent oversize to accommodate all excess metal, allowing the mating surfaces to close.

In terms of its contribution to the closed-die mechanical press forging processes, flash serves two basic functions [6]. First, by providing a convenient means for disposing of excess metal, it makes possible the use of slightly oversized billets and renders other billet dimensional variations, such as deviations in cutting to length or metal losses caused by oxidation during forging or heating of billet, much less critical. Availability of excess metal also increases possibility of the die filling. Second, flash provides useful constraint of metal flow during forging, which helps in filling the die impressions. Before complete closure of dies, the presence of some flash metal at the periphery of the workpiece promotes containment of the workpiece metal within the impressions.

While flash can promote complete fill of the cavity, it causes extremely high die pressures in the flash area. High pressures are undesirable because they reduce die life and require additional power. A flash gutter is often formed in the dies to receive the flash and allow the dies to reach the predetermined position at lower pressures.

## 1.2 Causes of Die Failure

The three basic cause of premature die failure are overloading of the die, wear and over heating [3].

### 1.2.1 Overloading of the Die

Although fewer die failure can be attributed to overloading than to wear or overheating, an overloaded die wear rapidly and may break. Overloading can be avoided by careful selection of die steel and hardness, use of blocks of adequate size, proper application of working pressure, proper die design to ensure correct metal flow, and proper seating of the dies in the hammer or press.

### 1.2.2  Wear on the Die

Wear is inherent in the flow and spreading of hot metal in the impression of a forging die. Wear is particularly severe if the design of the forging is complex or in other respects difficult-to-forge, if the metal being forged has a high hot strength, or if there is scale on the work metal.

Although wear cannot be eliminated, its effects can be minimized by good die design, including provision for a smooth progression in the shape of the forging from one die impression to the next, with work in the finisher at the minimum that is practical, careful selection of die composition and hardness, and a forging technique that includes proper heating, and necessary descaling, and correct die lubrication.

### 1.2.3  Overheating of the Die

As a die becomes hotter, its resistance to wear decreases. Over heating causes most of the premature die wear that occurs in forging. Overheating is likely to occur in areas of the die impression that project into the cavity. In addition, overheating may result from continues forging. If an internal die-cooling system that is adequate to prevent overheating cannot be provided economically, dies, or portions of dies that are susceptible to overheating should be constructed of steels with high heat resistance. Typical forging temperatures for various metals are shown in Table 1.1. Actual temperature may vary 50 $^{o}$C or more from those listed in Table.1.1, depending on the composition of the particular alloy being forged.

Since forging temperature typically range from 370 to 1260 $^{o}$C, temperature of the die block will also cover a broad range. In forging aluminum and magnesium alloys, it is desirable to maintain die temperature near the forging temperature of metal, to minimize the loss of heat from the forging. In forging steel, thin projections or plugs may reach 425 to 550 $^{o}$C, but the temperature within the die block usually is in the range from 150 to 350 $^{o}$C.

Table 1.1 Typical forging temperatures for various metals [3].

| Metals | Temperature($^{o}$C) |
|---|---|
| Magnesium alloys | 370 |
| Aluminum alloys | 425 |
| Cooper alloys | 800 |
| Tool steels | 1000 |
| Stainless steels and heat-resisting alloys | 1200 |
| Carbon and alloy steels | 1260 |

Dies for forging steel and other metals that must be forged at high temperatures are susceptible to heat checking [3], or the development of minute cracks in the die impression. Heat checking appears mainly in corners or on projections of the die. It occurs when the die surface has become overheated while the center of the block remains relatively cool. The variation in rates of contraction on cooling causes the surface to crack. Once cracks are started, forging forces (specially the forces of impact) will cause cracks to grow, and if this is allowed to continue, die breakage will result.

Most heat checking occurs in the forging of steel and heat-resisting alloys, considerably less in the forging of copper alloys, and little in the forging of aluminum or magnesium alloys, because of work-metal temperature. The possibility of heat checking is reduced when the die is lubricated or when an internal cooling system is used.

**1.3 Factors Affecting Die Life and Wear**

Die life depends on several factors, including die material and hardness, work-metal composition, forging temperature, condition of the work metal at forging surfaces, type of equipment used, and workpiece design.

Changing one factor almost always changes the influence of another, and the effects are not constant throughout the life of the die [3].

### 1.3.1 Die Material and Hardness

Die material and hardness have great influence on die life. A die made of well-chosen material at the proper hardness can withstand the severe strains imposed by both high pressure and heavy shock loads, and can resist wear, cracking and heat checking.

AISI H13, AISI L6 and DIEVAR [7, 8] are hot work tool steels that are commonly used for hot forging operations. The suggested hardness for hot forging operation tools for forging steel work pieces is between 45 and 55 HRC [9]. By applying complex heat treatment, higher hardness can be obtained on the surface of the die by formation of coated layer, white layer with 2-4 μm thickness, in order to increase the wear resistance of the die. The hardness of die can reach to 60 HRC on the surface of the die [10].

### 1.3.2 Workpiece Material

Each material being forged has a different resistance to plastic deformation and, therefore, a different wear action against the die surfaces. The resistance of hot steel to plastic deformation increases as the carbon or alloy content increases. Other factors being constant, the higher the carbon or alloy content of the steel being forged, the shorter the life expected from the forging die.

Of all the work-metal factors influencing die life, the temperature of the metal being forged is one of the most difficult to analyze. The surface temperature of the metal as it leaves the furnace can be determined, but unless the proper heating technique has been used, ensuring that the temperature is the same throughout the cross section, the measured temperature will not be an accurate indication of metal temperature. Cooling of the metal during the forging is accompanied by an increase in its resistance to plastic deformation and, correspondingly, in its abrasiveness.

The life of finisher impression can be increased by reheating the preform before finish forging. Even though the metal may be hot enough to forge satisfactorily without reheating, forging of cooled metal in the finisher impression may cause premature flash cooling and premature wear of the flash land.

When the temperature of the flash is reduced several hundred degrees and forging is continued, the cushioning effect that would be provided by freely flowing flash is either greatly reduced or lost completely. If the dies do not crack, they suffer a peening effect on the flash land, which may cause a bulge in the die impression.

### 1.3.3 Workpiece Design

The shape and design of the workpiece often have a greater influence on die life than any other factors. For instance, records in one plants showed that in hammer forging of simple round parts (near minimum severity), using dies made of 6G tool steel at 341 to 375 Bhn, the life of five dies ranged from 6000 to 10000 forgings. In contrast, with all conditions essentially the same except that the workpiece had a series of narrow ribs about 25 mm deep (near maximum severity), the life of five dies ranged from 1000 to 2000 forgings[3].

In thin section of a forging, the metal cools relatively rapidly. During cooling, it becomes to flow and causes greater wear on the die. Thin sections, therefore, should be forged in the shortest time possible. Draft angles in the die cavity, and correspondingly, draft on the part, increase as more forgings are made in the die. This is because wear on the die wall is greatest at the parting line, and least on the sidewall at the bottom of the cavity. Maximum wear near the parting line is caused by metal being forced to flow into the cavity, and then along the flash land.

Deep narrow depressions in a forging must be formed by high, thin sections in the die. The life of thin die sections usually is less than that of other die section, because the thin section may become upset after repeated use. Sometimes a minor change in forging design has a great influence on die life and on the number of acceptable forging produced.

### 1.3.4 Scale Formation

Steel forgings are coated on the surface with a thin layer of iron oxide or scale, which is caused by contact of the heated steel with air. Steel begins to oxidize at about 200°C; however, serious scaling, where substantial material may be lost and oxidized material spalls off the surface of the material, does not begin until the material reaches about 850°C [11]. The amount of scale that is formed depends upon the forging temperature to which the steel is heated and the length of time. The scale that is formed during the heating stage must be cleaned before putting the billet on the die, it helps to reduce die wear due to scale. Sometimes in the practice, the heated stock is being hammered or squeezed between the dies; hence, the formed scale begins to crack and separate from the forged material, and fall into the die. Because of this scale formation problem, a scale allowance has to be applied to the calculations of the billet volume. Bruchanow and Rebelski [12] recommended the values given in Table 1.2 for the calculation of scale allowance.

Table 1.2  Scale Allowance Values [12]

| Type of Furnace | Scale Allowance |
|-----------------|-----------------|
| Oil Box | 4% |
| Gas Box | 3% |
| Gas Continuous | 2.50% |
| Electric | 1.50% |
| Induction | 1% |

### 1.3.5 Required Workpiece Tolerance

Workpiece tolerance also has an influence on die life. Its effect on die life can be demonstrated by assuming a constant amount of die wear for a given number of forging, assigning different tolerances to a single hypothetical forging dimension, and then comparing the number of forging that can be made before the tolerances are exceeded. For instance, if a

dimension on a forging increased 0.025 mm during the production of 1000 forgings and the dimension had a total tolerance 0.75 mm, die life would be no greater than 30000 forgings, assuming a uniform rate of die wear. If the tolerance on the dimension were reduced to 0.5 mm, all other factors being the same, die life would be reduced to no more than 20000 forgings [3].

### 1.3.6 Rapidity and Intensity of Blow

The best die life is obtained when the forging energy is applied rapidly, uniformly and without excessive pressure. A single high-energy blow does not necessarily result in maximum die life. A blow that is too hard cause the metal to flow too fast and high pressure to develop on the die surface. Therefore, if all the energy needed to make a forging is applied in one blow, the dies may split. If the blows are softened, die wear due to pressure may decrease; but the increase in number of blows will add to forging time, and the additional time the hot metal is in contact with the lower die can decrease die life. The amount of heat transferred to the dies also can be reduced by stroking the press as rapidly as practical.

### 1.4 Modeling and Computer Simulation of Forging Operation

The design of dies and the selection of process conditions in forging operations are today still performed to a large extent by trial-and-error methods. In many cases, this trial-and-error procedure is neither optimal nor cost effective in terms of achieving the desired properties in the finished product. With the development of numerical analysis techniques, the finite element method was introduced in the early 1980's as a possible alternative. The finite element method has been extensively employed by several research groups but it is still not being readily implemented in the forging industry [13]. Hence, the finite element method cannot meet the highest standards for industrial acceptance [14], e.g.:

- The prediction of metal flow, stress, strain and temperature distributions requires accurate and robust algorithms. Since the process

of forging is typically characterized by gross 3-D material deformation and continuously changing boundary conditions, its complexity requires much simulator expertise and sometimes "tricks and tweaks" to produce a full solution.

- In order to optimize tool designs, the user must be able to perform parameter studies that require relatively short calculation times. However, finite element methods are relatively time consuming to use. Even rather simple 3-D applications can take several days on a workstation.

- Finite element meshes usually get over-distorted; auto-remeshing is then necessary to complete the simulation. But the auto-remeshing technology for three-dimensional problems is not so robust and also very time consuming [15].

- Even for two-dimensional elastic-plastic problems, the remeshing may lead to erroneous result [16]. Each remeshing step will involve quite a lot of loss in volume, which is not acceptable for forging simulations.

With the above challenges in mind, new soft wares started performing forging simulations with finite volume method, a 3-D analysis code for analyzing highly nonlinear, short-duration events involving the interaction of fluids and structures, or problems involving the extreme deformation of structural materials. It appeared that the finite volume method is well suited for 3-D forging simulations: MSC.Dytran which employs an explicit dynamics procedure in a finite element and finite volume method was selected by Sumitomo Heavy Industries to participate in a Japanese National Forging project [17].

### 1.4.1 Finite Volume Method (FVM)

The Finite Volume Method has been used for many years in analyzing the flow of materials in a liquid state. However, in recent years, some codes for computer simulation of solid state metal forming operations, such as MSC.SuperForge, have been established on the basis of this method. In the Finite Volume Method, the grid points are fixed in space and the elements are

simply partitions of the space defined by connected grid points. The finite volume mesh is a "fixed frame of reference." The material of a billet under analysis moves through the finite-volume mesh; the mass, momentum, and energy of the material are transported from element to element. The finite volume solver, therefore, calculates the motion of material through elements of constant volume, and therefore no remeshing is required [18].

### 1.4.2. Using MSC.SuperForge

MSC.SuperForge is a software package developed by MSC.Software Corporation for the computer simulation of 3D industrial forging processes. It combines a robust finite volume solver with an easy-to-use graphical user interface specifically designed for the simulation of 3D bulk forming operations. Forging companies and suppliers worldwide are effectively utilizing MSC.SuperForge to successfully simulate the forging of a variety of practical industrial parts.

By releasing of MSC.SuperForge Version 2000 a new Windows based graphical user interface is developed. Complex forging simulation models can now be set up in minutes, using familiar Windows drag & drop functionality. Once model setup is complete, the simulation can be started from within the user interface, and results can be visualized on the screen as the simulation progresses. Material flow can be visualized and animated with workpiece results such as stress, strain or temperature contours superimposed on the material flow animation. In addition, cut-sections can be animated, showing stress/strain/temperature results and potential folds inside the workpiece. Memory settings, workpiece-die interactions (contact), and finite volume domain generation are all fully automatic and require no user input or intervention [18]. Version 2004 of MSC.SuperForge provides new options as advance features for die analysis like die stress, die wear and die damage that make it possible to analyze die beside usual study of workpiece forging simulation [19].

Some previous studies have been conducted on different types of forgings by using finite elements and finite volume methods. Ceran [20]

studied on hot upset forging process by using a commercial finite element code coupled with thermal analysis in order to determine effects of the process on the header die for the taper pre-form stages. A study on upset forging process and the design limits for tapered preforms had been conducted by Elmaskaya [21] by using the elastic-plastic finite element method. Isbir [22] studied on the finite element simulation of shearing using the element elimination method to examine trimming operation on forged parts.

In the study of Doğan [23] the effects of the tapered preform shapes on the final product in cold upset forging had been investigated by using the elastic-plastic finite element method.

Alper [24] developed a computer program for axisymmetric press forgings, which designs the forging geometry and the die cavity for preforms and finishing operation. Kutlu [25] studied on the design and analysis of preforms in hot forging for non-axisymmetric press forgings. Karagözler [26] studied on the analysis and pre-form design for long press forgings with non-planar parting surfaces.

Gülbahar [27] used finite volume method to design perform workpiece and effect of perform design in flash generation; Civelekoğlu [28] analyzed the affect of different workpiece materials on hot forging operation.

**1.5 Scope of the Thesis**

As described in previous sections, the service life of dies depends so much on die wear, therefore wear analysis is an important matter for industry due to economical reasons. The wear process as a dynamic process depends on many parameters that make it so complicated for investigation. Fortunately in last decay so many codes have been established for computer simulation of solid state metal forming operations, by means of these developed codes, 3D simulation of forging process is possible.

In this study, the analysis of die wear will be focused. Results from computer simulation will be compared with the measurement on the worn die taken from industry and evaluation of wear coefficient from comparison of

computer simulation and the measurement from worn die will be done. Coordinate Measurement Machine (CMM) is used to model the preform workpiece and to do measurement on the worn die surface. Pro/ENGINEER is used for 3D modeling of the parts and mesh generation of the dies and the preform workpiece. Simulation of the forging process is preformed by using MSC.SuperForge.

Literature survey and recent studies are provided in Chapter 2. In Chapter 3, usage of CMM, CAD modeling and mesh generation of parts are explained. Case study is described in details in Chapter 4 and conclusions of this study will be presented in Chapter 5.

# CHAPTER 2

# LITERATURE SURVEY
# OF HOT FORGING DIE WEAR

Wear is the progressive damage, involving material loss, which occurs on the surface of a component as a result of its motion relative to the adjacent working parts; it is the almost inevitable companion of friction. Most tribological pairs are supplied with a lubricant as much to avoid the excessive wear and damage which would be present if the two surfaces were allowed to rub together in dry condition.

The economical consequences of wear are widespread and pervasive; they involve not only the costs of replacement parts, but also the expenses involved in machine downtime, lost production, and the consequent loss of business opportunities. A further significant factor can be the decreased efficiency of worn plant and equipment which can lead to both inferior performance and increase energy consumption.

The wear rate of a rolling or sliding contact is conventionally defined as the volume lost from the wearing surface per unit sliding distance. For a particular dry or unlubricated sliding situation, the wear rate depends on the normal load, the relative sliding velocity, and the thermal, mechanical, and chemical properties of the materials in contact. There are many physical mechanisms that can contribute to wear and certainly no simple and universal model is applicable to all situations. If the interface is contaminated by solid third body (for example, by entrained dirt or even just the retained debris from previous wear events) the situation can be much more complex. [29]

## 2.1 Classification of Wear

The simplest classification of surface interactions is into those involving either *mild* or *severs* wear. This classification is not really based on any particular numerical value of wear but rather on the general observation that, for any pair of materials, increasing the severity of the loading (e.g. by increasing either the normal load, sliding speed, or bulk temperature) leads at some stage to a comparatively sudden jump in the wear rate. The generally observable differences between the two regimes of mild and severe wear in a variety of sliding metallic systems are summarized in Table 2.1.

Table 2.1. Distinction between mild and sever wear [31].

| Mild wear | Severe Wear |
| --- | --- |
| Results are extremely smooth | Results in rough, deeply torn |
| Surfaces- often smoother than original | Surfaces- much rougher than the original |
| Debris extremely small. Typically only 100 nm diameter | Large metallic wear debris, typically up to 0.01 mm diameter |
| High electrical contact resistance, little true metallic contact | Low contact resistance, true metallic junctions formed |

One way of exploring wear broad pattern, and of indicating the way in which changes in the service conditions can influence the material wear response, is to construct an appropriate map of wear behavior. Two approaches are possible, one is empirical: mechanism maps are built up by plotting experimental data for wear rates on suitable axes, identifying at each point the mechanism by direct experimental observation. The other uses physical modeling: model-based equations describing the wear rate for each mechanism are combined to give a map showing the total rate and the field of operation within which each is dominant. An immediate difficulty is the choice of the most appropriate coordinate axes on which to display the chosen data. The general form of such a map is illustrated in Figure 2.1, and various regimes of wear are identified [30].
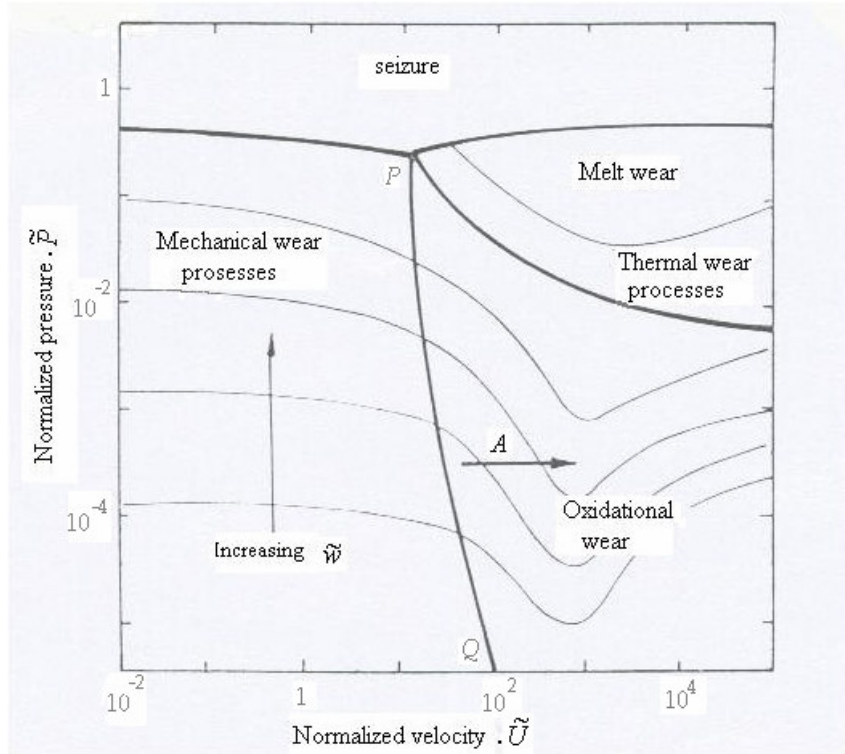
Fig.2.1. Wear map for steel using a pin-on disc configuration [29].

Figure 2.1 shows the essential features of a load-speed wear map for steel using a pin-on disc configuration. Load and speed have both been normalized. Thick lines delineate different wear mechanisms and thin lines are contours of equal $\tilde{w}$.

In Figure 2.1 pressure, speed, and wear rate have each been expressed non-dimensionally by using the relations

$$\tilde{P} = \frac{P}{H} \tag{2.1}$$

$$\tilde{U} = \frac{U}{a} \cdot \sqrt{\frac{A_{nom}}{\pi}} \tag{2.2}$$

$$\tilde{w} = \frac{w}{A_{nom}} = K \cdot \tilde{P} \tag{2.3}$$

where $P$ is normal contact pressure (Pa), $\tilde{P}$ is (non-dimensional) normalized pressure, $H$ hardness (Pa), $U$ relative sliding velocity (mm/sec), $\tilde{U}$ (non-dimensional) normalized velocity, is the thermal diffusivity of the wearing

19

material and is equal to the value of the thermal conductivity divided by the product of the density and specific heat, $A_{nom}$ is nominal contact area (mm$^2$), $w$ is volume of wear in sliding distance (mm$^3$/mm), $\tilde{w}$ is (non-dimensional) normalized wear and $K$ is non-dimensional wear coefficient.

Region of the map associated with different wear mechanisms are traversed by contours of equal normalized wear rate $\tilde{w}$. It can be seen that the total area is roughly divided into two regions by the line *PQ*. To the left of this divide, wear is controlled essentially by mechanical processes; here the wear rate depends on the normal pressure (or load) but is not greatly dependent on sliding velocity. On the other hand, to the right of *PQ*, thermal (and chemical, particularly oxidational) effects become the dominant influence and contours of $\tilde{w}$ become functions of both load and velocity. The transition from mild to severe wear occurs when the contours of $\tilde{w}$ have a steep slope, for example at arrow *A*.

## 2.2 Mechanisms of Wear

### 2.2.1 Seizure

When metal surfaces are brought into contact the real area over which they touch is a comparatively small fraction of the nominal contact area. The high normal pressure generated at these asperity contacts forge metallic junctions which, when they are sheared by the application of a load tangential to the interface, can grow until actual area of metallic contact approaches the nominal area; this is the phenomenon of 'junction growth'. The behavior of an individual asperity contact can be described by a relationship of the form [30]:

$$P^2 + \alpha_1 \cdot \tau^2 = \alpha_2 \cdot \psi^2 \qquad (2.4)$$

In this equation $P$ is the normal pressure at the asperity, $\psi$ the bulk shear strength of the solid, and $\tau$ the interfacial shear strength; $\alpha_1$ and $\alpha_2$ are constants. When $\tau / \psi = 0$, the pressure $P$ is equal to material hardness $H$,

$$H = \sqrt{\alpha_2} \cdot \psi \qquad\qquad (2.5)$$

When at the limit $\tau / \psi$, that is, the friction factor *m,* approaches the value unity, the normalized pressure $\tilde{P}$ $(=P/H)$ is given by

$$\tilde{P} = \sqrt{1 - m^2 \cdot \alpha_1 / \alpha_2} \qquad\qquad (2.6)$$

Setting both value of *m* and the ratio $\alpha_1/\alpha_2$ equal to 0.9 (values consistent with observation) suggests a value of *P* between 0.5 and 0.6, which will be independent of the sliding speed parameter *U*. this argument is consistent with the simple straight boundary between sliding and seizure conditions on a wear map (Figure 2.1).

### 2.2.2 Melt Wear

Localized melting of the uppermost layer of the wearing solid is always a possibility; evidence for its occurrence has been found in wear tests on steels even at sliding speeds as low as 1 m/sec [30]. At higher velocities the coefficient of friction can drop, eventually to very low values, as a film of liquid metal forms at the interface which acts in the same way as a hydrodynamic lubricating film. The heat generated by viscous work in such a 'melt lubrication' situation continues to melt more solid so that the wear rate can be high despite the fact that the coefficient of friction is low. The metal removed from the surface can be ejected as sparks or incandescent debris, or even in extreme cases, squirted out as a molten stream. This leads an Equation of the form [30],

$$\tilde{w} = \eta_1 \cdot \tilde{P} - \frac{\lambda_1}{\tilde{U}} \qquad\qquad (2.7)$$

$\eta_1$ and $\lambda_1$ are in form of

21

$$\eta_1 = \frac{\alpha \cdot \mu \cdot H_0}{L} \tag{2.8}$$

$$\lambda_1 = (\frac{T_m - T_0}{T^*}) \cdot \frac{H_0}{L \cdot \beta} \tag{2.9}$$

where

$\alpha$ : Heat distribution coefficient between bodies in steady state condition is equal to 0.5

$\mu$ : Coefficient of friction

$H_0$ : Hardness of steel in steady state condition (Pa)

$L$ : Latent heat of fusion per unit volume for metal (J/m$^3$)

$T_m$ : Melting temperature of metal (K)

$T_0$ : Sink temperature of bulk heating (K)

$T^*$ : An equivalent temperature for metal (K)

$\beta$ : Dimensionless parameter for bulk heating

When the velocity of sliding is low then the second term of Equation 2.5 becomes large, so that wear is small; at high sliding velocities the first term of Equation 2.5 becomes of greater significance and the wear characteristics fan out as indicated in the top right-hand section of Figure 2.1.

### 2.2.3 Oxidation-dominated Wear

Figure 2.1 includes a large region at higher speeds designated 'oxidational wear'. The existence and extent of this regime, and the wear rates within it, are dependent on the ability of the wearing material to undergo oxidation and, equally of course, on the availability of oxygen in the immediate vicinity of the sliding contact.

When dry steel surface slide at speeds below about 1 m/s the wear debris is largely metallic; at higher speeds it consists mainly of iron oxides [32]. A velocity of 1 m/s (which translates to a normalized velocity value of about 100) is just sufficient to give flash temperatures $T_{flash}$ sufficient to cause oxidation, that is, of about 700 $^\circ$C. The value of $T_{flash}$ is strongly dependent on

velocity but varies hardly at all with load, hence the near verticality of the boundary PQ in Figure 2.1. The presence of an oxide film at the interface may be sufficient to reduce the wear rate merely by its role of suppressing or at least reducing, the degree of the mechanical interaction. Close to the line PQ the oxide film is thin, patchy, and brittle, and wear is caused largely by its splitting off form the surface. This spalling away exposes more metal which rapidly oxidizes once again. This regime known as mild oxidational wear which is of the form [33]

$$\tilde{w} = c \cdot \exp\{-\frac{Q_0}{R \cdot \mathrm{T_{flash}}}\} \times \frac{\tilde{P}}{\tilde{U}} \qquad (2.10)$$

$Q_0$ (J/mol) can be taken as the activation energy for the static oxidation of iron and $R$ (J/mol.K) is the universal molar gas constant, but the constant $c$ must be established empirically.

Higher sliding velocities generate higher temperature; not only do oxidation rates consequently increase but also now the resulting oxide film may begin to soften and deform locally, absorbing latent heat as it does so. The film in this region of severe oxidational wear subsequently flows and spreads out over cooler region of the surface so effectively this energy as the oxide solidifies. Asperity melting is thus a way of redistributing this energy as the heat input to the surface in a more uniform way. By making sensible idealization about the nature and severity of asperity contact it has proved possible to tentatively outline a model which has the general form [30]

$$\tilde{w} = f_m \times \left\{ \eta_2 \cdot \tilde{P} + \lambda_2 \frac{\sqrt{\tilde{P}}}{\tilde{U}} \right\} \qquad (2.11)$$

$\eta_2$ and $\lambda_2$ are in form of

$$\eta_2 = \frac{\alpha \cdot \mu \cdot H_0}{L_{ox}} \qquad (2.12)$$

$$\lambda_2 = -\frac{K_{ox}(T_m{}^{ox} - T_b) \cdot N^{\frac{1}{2}}}{L_{ox} \cdot a \cdot \beta} \qquad (2.13)$$

where

$f_m$ : a factor which accounts for the proportion of the molten oxide which is lost from (rather than being distributed over) the surface.

$K_{ox}$ : Thermal conductivity of oxide (J/m.s.K)

$L_{ox}$ : Latent heat of oxide melting (J/m$^3$)

$T_m{}^{ox}$ : Melting point for oxide ($^o$K)

$T_b$ : Bulk temperature of surface ($^o$K)

$a$: Thermal diffusivity of metal (m$^2$/s)

$N$ : Number of contacting asperities

### 2.2.4 Mechanical Wear Processes

At normalized velocities below about 10 (equivalent in the case of steels to actual velocities less than 0.1 m/s) surface heating is negligible; the effect of the frictional force is principally to deform the metal surface, shearing it in the sliding direction and ultimately causing the removal of material usually in the form of small particles of wear debris. In this regime the wear behavior often follows the Archard [34] equation

$$w = K \times \frac{F_N}{H} \qquad (2.14)$$

where $F_N$ is normal load on contact interface (N).

The aim of any model of the process is to predict the wear coefficient $K$ in terms of material and process parameters. Since now velocity plays only a minor part in the argument.

### 2.2.4.1 Running-in

When mass produced lubricated machine components are run together for the first time their ultimate load-carrying capacity is often very much less than would be the case if they had been preconditioned by running together for an initial period at a comparatively light load. This process, during which they improve in conformity, topography, and frictional compatibility, is known as running-in.
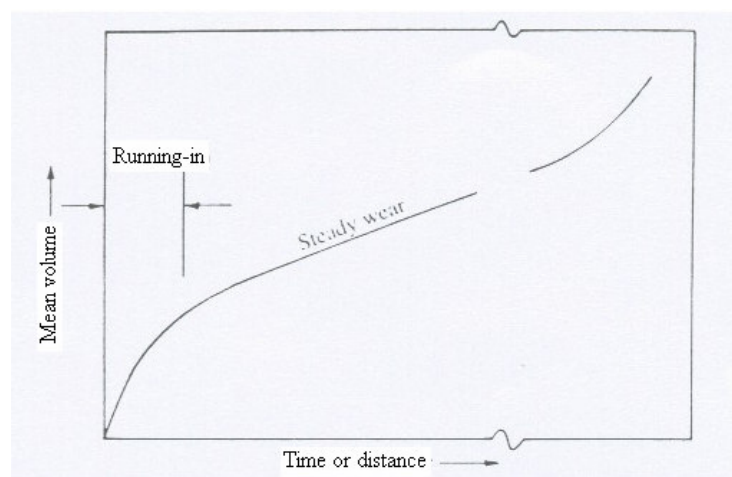


Fig.2.2. Typical wear behavior over the life of a component [29].

During running-in a number of mechanical wear processes, especially those that depend on adhesion and abrasion, are likely to be operating simultaneously. Once running-in is complete the steady low-wear-rate regime is maintained for the operational life of the component; the wear rate rises again once the operating time becomes sufficiently long for fatigue processes in the upper layer of the loaded surface to start making a significant contribution to material loss driven by the cyclic nature of the component loading.

### 2.2.4.2 Adhesive Wear

Models of adhesive wear have a long pedigree-they are all based on the notion that touching asperities adhere together and that plastic shearing of the junctions so formed 'plucks' off the tips of the softer asperities leaving them adhering to the harder surface. Subsequently these tips can become detached giving rise to wear particles or fragments. Sever damage of this type can result in the tearing of macroscopic chunk of material from the surface and this situation is sometimes known as galling. It can be a particular problem when both members of the tribological contact are made of the same sort of material (e.g. both of ferrous alloy) or when there is poor lubrication and temperature or sliding speeds are high. The term scuffing is used specially to describe the onset of adhesive wear between lubricated surfaces which has arisen from the break down or failure of the lubricant film for whatever reason.

The simplest situation and that considered by Archard, is illustrated in Figure 2.3, which shows a single asperity junction of diameter 2a. For a wear particle to be formed, shearing of the junction AB must occur along some path such as path 2, rather than along the original interface path 1.
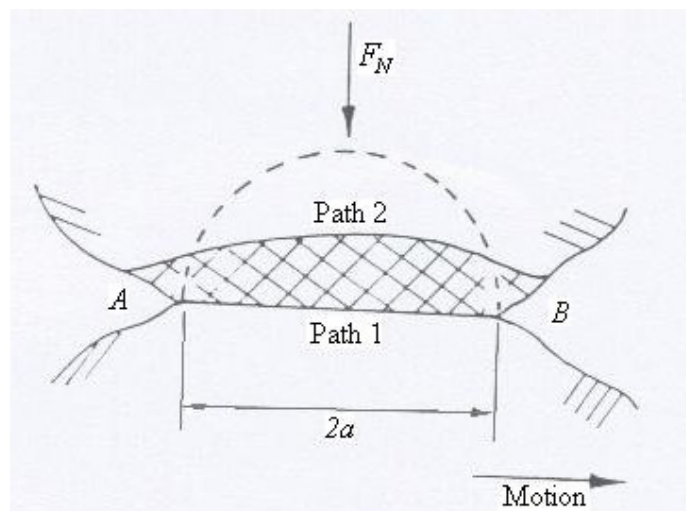
Fig.2.3. Production of a wear particle by adhesion [29].

26

Even at first sight this would seem to be a relatively rare event, since the original contacting interface is likely to have both the smallest cross-sectional area and the highest density of defects, and so represents the path of lest resistance [29]. However, on occasion, particularly if the asperities interact so that the plane AB in inclined to the sliding direction, a transferred particle can be formed. Archard model is formed as:

$$w = K_{adh} \times \frac{F_N}{H} \tag{2.9}$$

Where $w$ is volume of wear per sliding distance (mm$^3$/mm), $K_{adh}$ is non-dimensional adhesive wear coefficient, $F_N$ is normal contact load (N) and H is hardness (Pa).

Support of such simple models of adhesive wear, which suggest that material is removed or plucked from asperities on the wearing surface, is provide by those cases in which the wear debris is found to have an irregular, or 'blocky' shape of dimensions which seem appropriate to the surface in question. Although examination of the debris can give valuable clues to the mechanisms of its production it is always important to question whether the debris particles are in the same state when they are collected as when they were first produced or detached. They may, for example, have been further plastically deformed by rolling between the surfaces or have been changed by oxidation.

### 2.2.4.3 Abrasive Wear

Abrasive wear is damage to a component surface which arises because of the motion relative to that surface of either harder asperities or perhaps hard particles trapped at the interface. Such hard particles may have been introduced between the two softer surface as a contaminant from the out side environment, or they may have been formed in situ by oxidation or some other chemical or mechanical process. On the other hand, abrasion may take place simply because the counter face is both rough and essentially harder than the

wearing component. If wear depends on the presence of free particles the situation is known as three-body abrasion; if the wear producing agent is the hard counterface itself we have two-body abrasion.

Abrasive wear gives a characteristic surface topography consisting of long parallel grooves running in the rubbing direction. The volume and size of the grooves varies considerably from light 'scratching' at one extreme to severe 'gouging' at the other and industrial surveys invariably indicate that abrasive wear account for up to about 50 percent of wear problems.

Attempt to develop a model of abrasive wear nearly always assume that the deformation of the harder surface are negligibly small compared to those of the softer member and have concentrated on the effect of a single isolated hard asperity moving across a softer previously undeformed surface. Consider, for example, the very simple situation illustrated in Figure 2.4. which shows a conical asperities with semi angle $90^o$ - $\theta$ carrying a normal load $F_N$ so that it indent the soft surface to depth $h$ the angle $\theta$ represent, by extension, the 'average' surface slope or roughness of the abrading surface which might carry an array of such asperities.
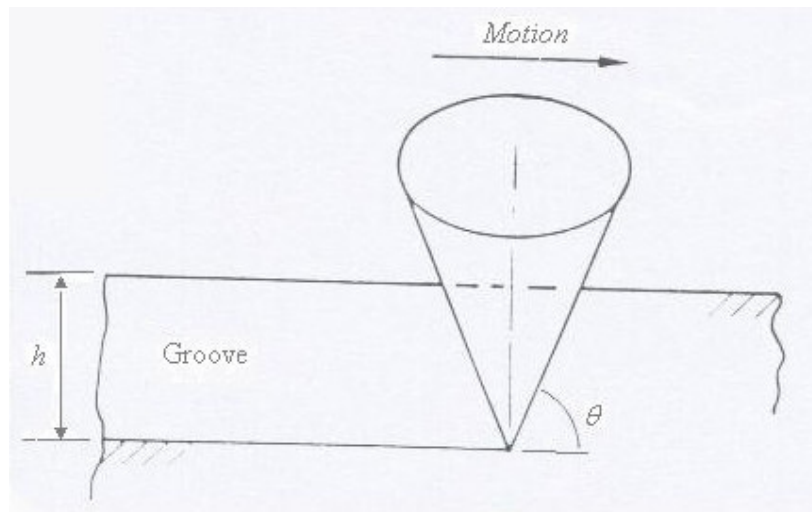


Fig.2.4.  A single conical asperity moving through a soft surface [24].

Abrasive wear in practice can often be described by an equation of the same form as Archard wear equation:

$$w = K_{abr} \times \frac{F_N}{H} \qquad (2.16)$$

where $K_{abr}$ is non-dimensional abrasive wear coefficient.

The volumetric loss of material in a given situation is proportional to the distance slid and the intensity of the loading. If we define the abrasive wear resistance of a material as simply the inverse of the wear volume we should expect this quantity to be proportional to the hardness $H$. the classical experiments confirmation of this effect was carried out in many experimental observations (Kruschov [35]) since 1950's.

## 2.3 Recent Studies of Hot Forging Die Wear Analysis

Several researches have been done on wear phenomenon of hot forging operation including the wear model and, wear prediction, wear reduction, etc. In hot forging process main appearance of wear is due to mechanical wear mechanism. Conditions like high pressure (close to hardness of die material), high sliding velocity (over 1 m/sec) and flash temperature (over 700$^{o}$C) that cause other wear mechanisms such as melt wear and oxidation wear, hardly appears during operation, although oxidation wear may appear on flash land due to high sliding velocity. Then mechanical wear mechanism seems to be appropriate for hot forging operations wear analysis.

General Archard's [34] wear model has been applied to predict die wear in most of hot forging process studies. The amounts of wear, as explained, are proportional to the wear coefficient between the die and the workpiece, the surface pressure of the die, the relative length movement between the die and the workpiece and inverse to the hardness of the die. The surface pressure and relative sliding length can be obtained from computer simulation using commercial codes. Hardness of die material in operation conditions can be found from metal hand books, in special cases like high temperature or

different heat treatments, hardness test can be done for better results. The non-dimensional wear coefficient is introduced to provide agreement between theory and experiment, it has great influence on result of wear, its value changes for different materials in contact and different conditions (Table.2.2) therefore it is not possible to offer a certain value of wear coefficient for different contact problems.

Table 2.2 Typical values of dimensionless wear coefficients for various materials against tool steel sliding in dry, unlubricated pin-on-disc tests in air [34].

| Material | $K$ |
|---|---|
| Mild steel (on mild steel) | $7 \times 10^{-3}$ |
| $\alpha/\beta$ brass | $6 \times 10^{-4}$ |
| PTFE | $2.5 \times 10^{-5}$ |
| Copper-beryllium | $3.4 \times 10^{-5}$ |
| Hard tool steel | $1.3 \times 10^{-4}$ |
| Ferritic stainless steel | $1.7 \times 10^{-5}$ |
| Polythene | $1.3 \times 10^{-7}$ |
| PMMA | $7 \times 10^{-6}$ |

The most used method for obtaining wear coefficient is pin-on-disk or ring-on-disk tests, by knowing sliding length, material properties, normal contact pressure and volume of material lost, wear coefficient can be calculated in form of

$$K = \frac{\Delta V \cdot H}{L \cdot F_N} \qquad (2.17)$$

where $K$ is non-dimensional wear coefficient, $\Delta V$ is measured wear volume ($mm^3$) and $L$ is the sliding length (mm).

Sobis [37] studied the real contact areas for wear prediction that is the limits of the Archard's model. Painter [38] analyzed the die wear in the hot extrusion using the finite element code DEFORM to simulate the process and wear program to predict the wear condition. Lee and Im [39] also used the finite element method to investigate the wear and elastic deformation of die. In this study the value of $K$ is taken in the order of $10^{-4}$ at the sliding interface of the workpiece and the die. Lim and Ashby [30] calculated wear coefficient regarding the delamination or plasticity dominated wear mechanism as governing. For steels they suggested to use the values:

$$K = 5 \times 10^{-5} \qquad \text{if} \quad \tilde{P} \langle 3 \times 10^{-4}$$

$$K = 5 \times 10^{-3} \qquad \text{if} \quad \tilde{P} \rangle 3 \times 10^{-4}$$

In a study by Podra [40], dimensional wear coefficient $k$ ($Pa^{-1}$), which is equal to non-dimensional wear coefficient $K$ over die hardness $H$, is used for calculating wear. Value of dimensional wear coefficient was obtained from wear test. Unlubricated pin-on-disc experiments were made at room temperature with a spherical steel pin with a radius of $R$=5 mm sliding on a steel disc with normal load $F_N$=21 N or $F_N$=50 N. The discs and the pins were hardened to $HV$=4.6 GPa and $HV$=3 GPa, respectively. From the Hertz contact pressure distribution, for the normal force of $F_N$=21 N the maximum contact pressure is 1200 MPa and the average contact pressure is 800 MPa and for $F_N$=50 N, the maximum contact pressure is 1650 MPa and the average contact pressure is 1100 MPa. The sliding velocity in the tests was $U$=25 mm/s.

The overall average dimensional wear coefficient were computed from both test series as $k$=(1.33±0.54)·$10^{-13}$ $Pa^{-1}$ and $k$=(2.01±1.21)·$10^{-13}$ $Pa^{-1}$ for the sliding distances L=3 m and L=4.5 m respectively (Figure 2.5).

$F_N=21 N$        $F_N=50 N$
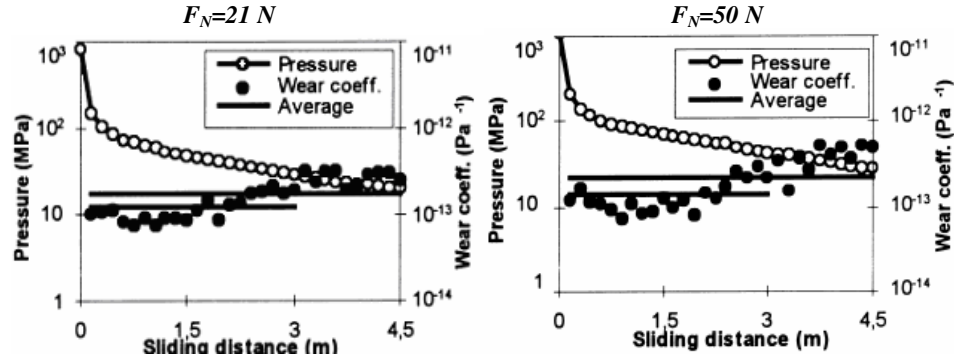
Fig. 2.5 Pin-on-disc experiment data for steel as a function of sliding distance [40].

Recently, Kang [10, 41] proposed a new wear model considering thermal softening of die material and used it to calculate the wear profile of a rotor pole for automobile warm forging die. In this study wear tests of pin-on-disk type has been done to acquire the die wear coefficient. Tests have been done for six types of heat-treated to measure the wear coefficient of actual heat-treatment used in industry. Two value of wear coefficient are obtained, at the beginning of operation when coated layer of die is in contact with workpiece, wear coefficient is equal to $0.74 \times 10^{-6}$. While depth of wear, $d$ (mm), exceeds 4 μm wear coefficient must be changed into that of diffusion layer below coated layer, $1.33 \times 10^{-6}$ (Figure 2.6).

Die's material has been subjected to quenching, tempering and 15, 30, 45 and 60 hours of nitriding, were reheated to 600°C, 625°C and 650°C for 20, 40 and 60 hours. Die material softening related to time and temperature was measured using a Vickers hardness tester and converted to the Rocwell C scale (HRC). The tempering softening curve can be expressed as

$$H = A \cdot \exp(B \times (M \times 0.001)^C) + D \qquad (2.18)$$

where *A, B, C* and *D* are die softening constants and *M* is tempering parameter as $M = T_{temper}(20 + \log t)$, where *t* is tempering time (h) and $T_{temper}$ is the tempering temperature (K). The suggested wear model is in form

32

$$d = K(d) \times \frac{P \times L}{H(T_{temper}, t)} \qquad (2.19)$$

where $d$ is depth of wear (mm), $K$ is non-dimensional wear coefficient obtained from wear test, $P$ contact normal pressure (Pa), $L$ sliding length (mm) and $H$ harness, temperature $T_{temper}$ (K) and tempering time dependent $t$ (h).
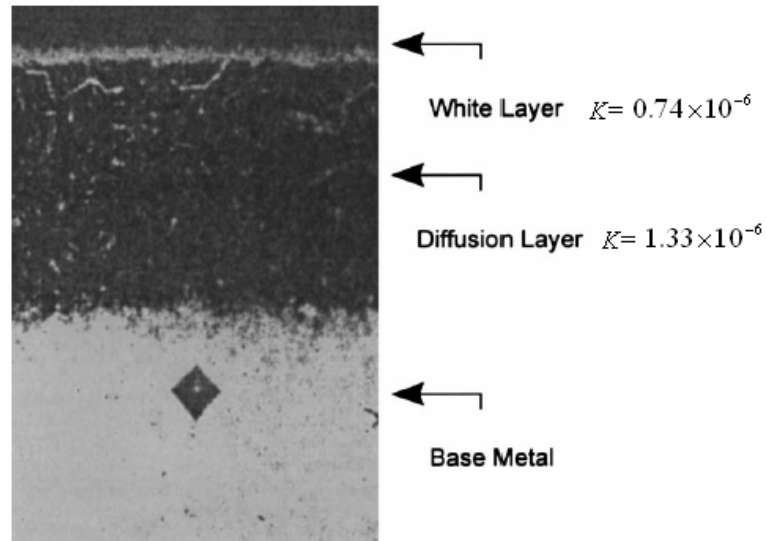


Fig. 2.6 The layers of the nitride die [10].

Equation 2.13 can be modified to obtain the final amount of wear from one finite-element analysis.

$$d_{fin} = \sum_{1}^{n} K(d) \times \frac{P \times L}{H(T, t)} \qquad (2.20)$$

where $d_{fin}$ is final depth of wear in a point after $n$ times forging.

In other study by Lee [42], high temperature ring-on-disc wear test has been done to acquire the die wear coefficient. In the wear test, the disc is made of JIS SKD61 (AISI H13) die steel and the ring is made of JIS SKD51 high speed steel. The sliding velocity is 0.56 m/sec and the average contact pressure is 2.35 MPa, 300 N normal force is applied to 127 mm$^2$ contact area. The value of non-dimensional wear coefficient obtained about $2.5 \times 10^{-4}$ (Figure 2.7). The proposed wear model is expressed as Equation 2.21, where the wear coefficient $K$ and hardness $H$ are function of temperature:

$$d(T) = K(T)\frac{P \times L}{H(T)} \tag{2.21}$$
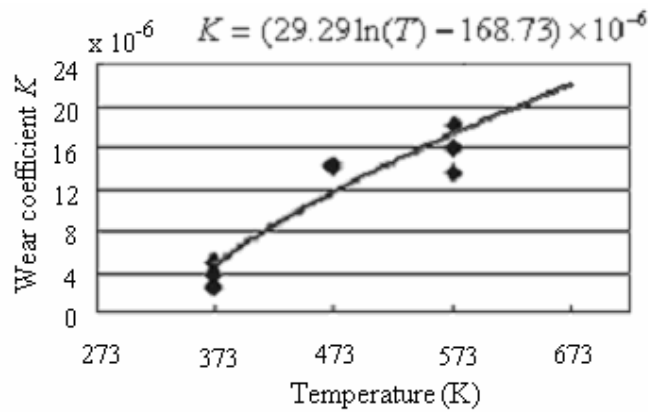


Fig.2.7. Wear coefficient acquired from test [42].

The hardness function of temperature $H(T)$ is acquired from the high temperature hardness test. The results are shown in Figures 2.8.

During forging, on the contact interface the pressure, temperature, velocity field are varying with position and time. Therefore, Equation 2.21 can be written in form of

$$\Delta d_{ij} = K_{ij}(T)\frac{L_{ij} \times P_{ij}}{H_{ij}} \tag{2.22}$$

34

where $d_{ij}$ is wear depth of $i$th position of die in $j$th period $\Delta t_j$. Sliding length $L_{ij}$, pressure $P_{ij}$ and temperature $T$ can be acquired from forging process simulation by finite element or finite volume methods.
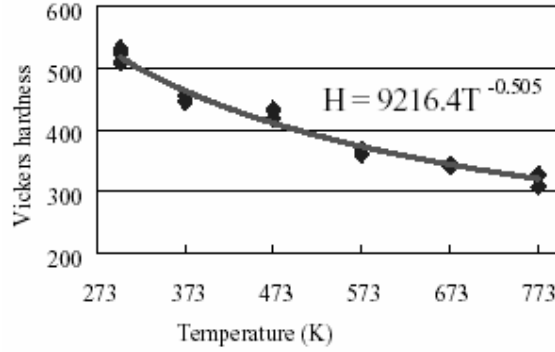


Fig. 2.8  Effect of temperature on hardness [42].

The wear depth of $i$th position of die in one forging can expressed as

$$d_i = \sum_{j=1}^{j=n} K_{ij}(T)\frac{L_{ij} \times P_{ij}}{H_{ij}(T)} \tag{2.23}$$

where $d_i$ is depth of wear end of one forging operation, $n$ is the total steps of the forging process simulation. From the wear distribution of all tracking position of the die, the wear profile can be predict after one forging process, and the final wear distribution or the life of the die can be obtained by summing up wear of all forging processes.

# CHAPTER 3

# THE WORN DIE MEASUREMENT AND
# MODELING OF THE WORKPIECE

This chapter includes preprocess of the wear analysis of the case study, that is, surface measurement of the worn die and the preform workpiece by using Coordinate Measurement Machine (CMM), also modeling of the preform workpiece by help of CAD software and using result of surface measurement.

The case study of this thesis is currently being performed in AKSAN Forging Company [8]. This part is forged in there forging steps as shown in Figure 3.1. Before starting the forging process, billets are prepared in the length of 125 mm with diameter of 70 mm (Figure 3.1-1). Material of the workpiece is X20Cr13 steel, which is equivalent to DIN 1.4021. These prepared billets are fed into the heater to reach the temperature of $1100^{o}$C. Material of the die is AISI L6 tool steel, which is equivalent to DIN 1.2714. Before starting the forging process, the dies are heated to $300^{o}$C in order to
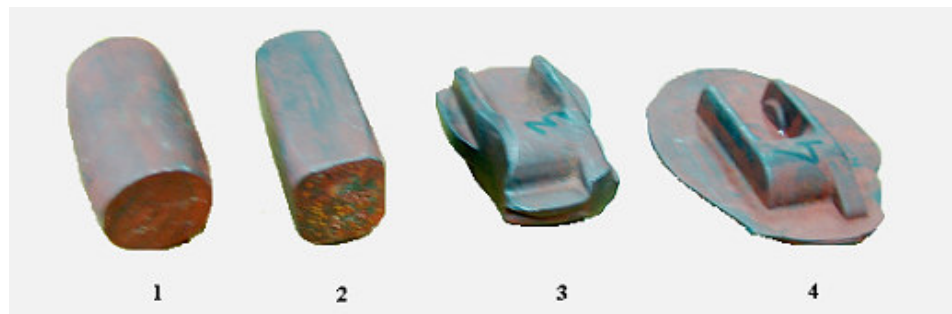


Fig 3.1 Different steps of the forging operation..

36

prevent die failure due to thermal stress. For the forging operation "1600 tonf" mechanical crank press is used. The wear analysis will be done for the finishing die which is important for final production quality.

### 3.1 Measurements by Using CMM

Measurements have been done in METU-CAD/CAM/Robotic Center. The Coordinate Measuring Machine available is model of PC-DMIS. This model for Windows is a full-featured, geometric measurement package. It translates the high-level commands required to measure parts into the detailed steps necessary to drive a Coordinate Measuring Machine (CMM). The parameters that are used for measurement are shown in Table. 3.1. The method of surface measurement is explained in Appendix A.

Table 3.1 The parameters used for surface measurement.

| Maximum Increment in Direction 1 | 3 mm |
|---|---|
| Minimum Increment in Direction 1 | 0.5 mm |
| Increment in Direction 2 | 5 mm |
| Maximum Angle | 5 |
| Minimum Angle | 0.5 |
| Move Speed | 50% |
| Touch Speed | 5% |

By using surface measurement method the coordinate measurement of die and pre-form workpiece has been done. As shown in Figure 3.2 the measurement of die is in form of parallel curves of different sections.

Result of preform workpiece measurement must be used in CAD program to make solid model, for this reason the output result of workpiece measurement is in form of measured points (Figure 3.3). By exporting data points to CAD program it is possible to draw smooth curves through the points and obtain a solid model. If the result of workpiece measurement exports to

37

CAD program was in measured curves instead of points, during solid modeling of part errors would occur due to roughness of imported curves from measurement and it is not possible to generate solid model of preform workpiece.
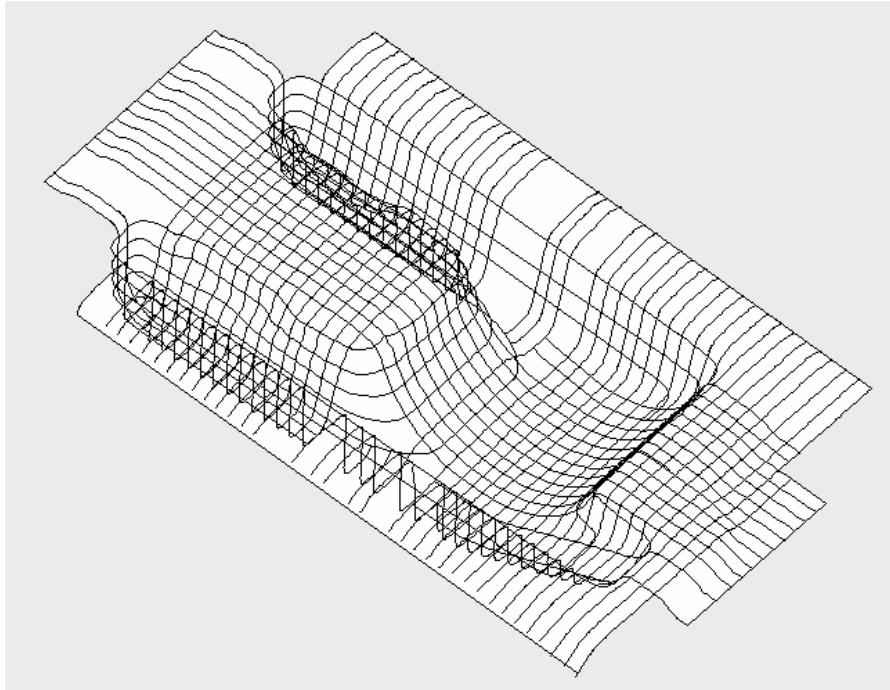


Fig. 3.2 Result of the worn die surface measurement.
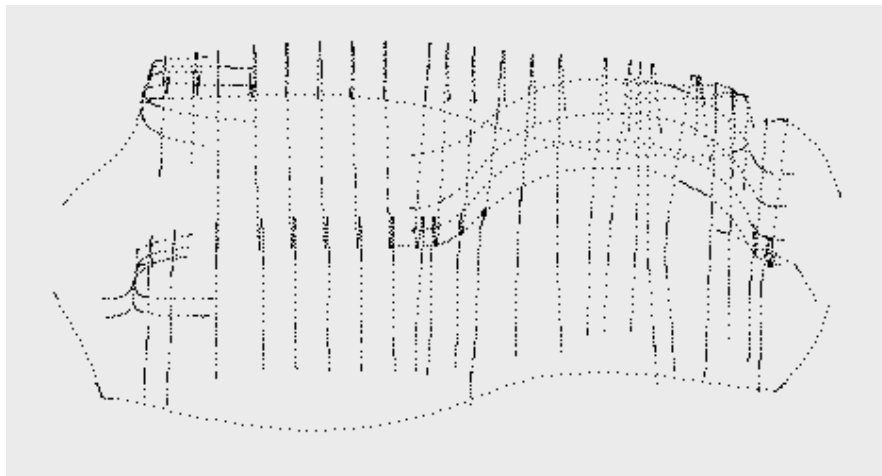


Fig. 3.3 Result of point tracking on the preform workpiece surface.

### 3.2 Modeling of the Parts

After measurements, the output results would be imported to CAD program for surface generation and solid modeling. In this study, Pro/Engineer is used for computer modeling of parts.

Pro/ENGINEER is a suite of programs that are used in the design, analysis, and manufacturing of a virtually unlimited range of products. Pro/ENGINEER is a parametric, feature-based solid modeling system [43].

Feature-based means that it is possible to create parts and assemblies by defining features like extrusions, sweeps, cuts, holes, slots, rounds, and so on, instead of specifying low-level geometry like lines, arcs, and circles. This means that the designer can think of his computer model at a very high level, and leave all the low-level geometric detail for Pro/E to figure out. Features are specified by setting values of attributes such as reference planes or surfaces, direction of creation, pattern parameters, shape, dimensions, and others.

Parametric means that the physical shape of the part or assembly is driven by the values assigned to the attributes (primarily dimensions) of its features. It is possible to define or modify a feature's dimensions or other attributes at any time. Any changes will automatically propagate through your model. It is also possible to relate the attributes of one feature to another. For example, if a new engine is designed, the diameter of the cylinder will automatically change if you change the diameter of the piston.

Solid Modeling means that the computer model created is able to contain all the information that a real solid object would have. It has volume and therefore, if you provide a value for the density of the material, it has mass and inertia.

By using advantages explained above Pro/ENGINEER will be used for modeling of parts. After obtaining points measured from preform workpiece

by CMM, first step is to pass curves through points in parallel sections. The result of this process is shown is Figure 3.4. Since the workpiece has plan symmetry the modeling can be done for half of the workpiece and at the end mirror the symmetry part. For creating solid, a close surface must be defined; therefore in this step a close surface will be created. For this propose between each curves in neighbors a surface will be create and at the end by merging surfaces to each other a close surface over the workpiece can be obtained.
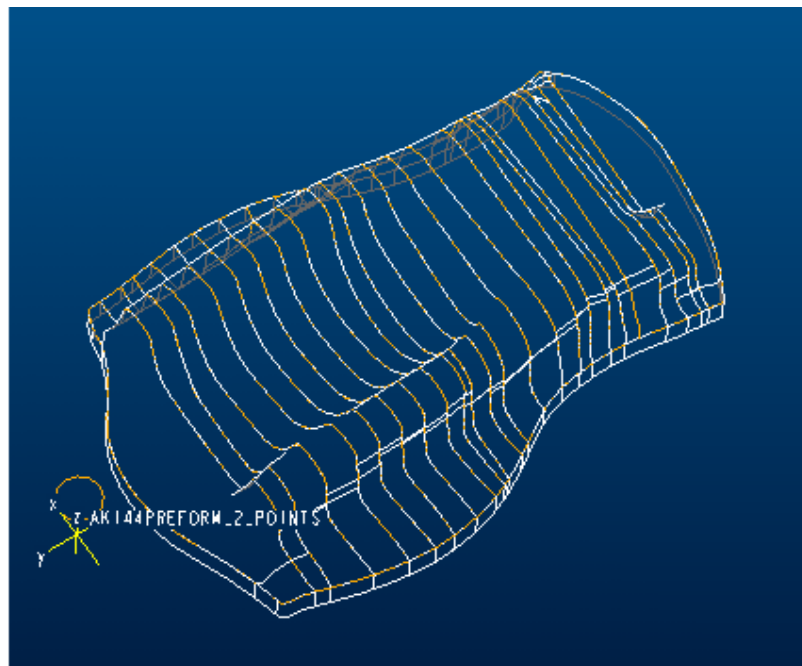


Fig. 3.4 Smooth curves passed through the measured points by CMM.

By using this close surface, it is possible to create a solid model. The solid model obtained is shown in Figure 3.5. By using symmetry plan as mirror the other half of workpiece can be obtained easily.

40
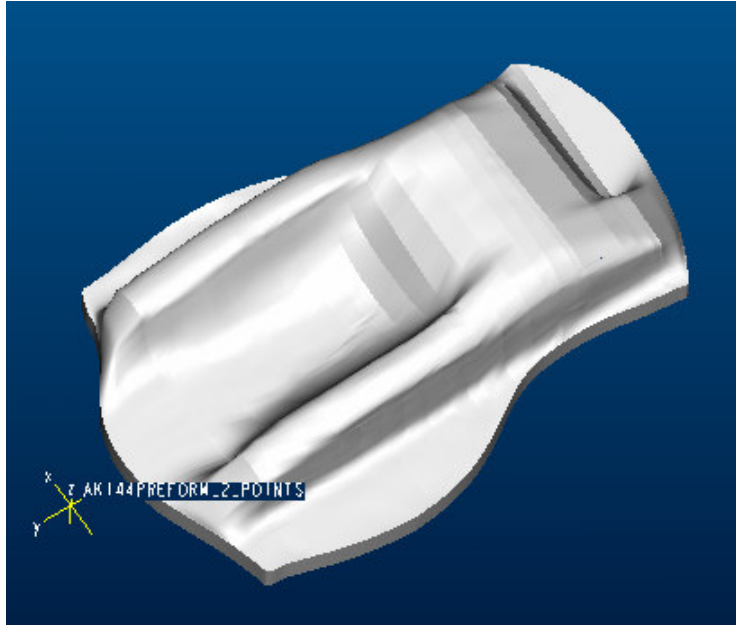
Fig. 3.5 Half-symmetry solid model of the preform workpiece.

The solid model of the die for the hot forging operation has been designed from previous study in METU-CAD/CAM Center, Figure 3.6 shows the solid model of die.
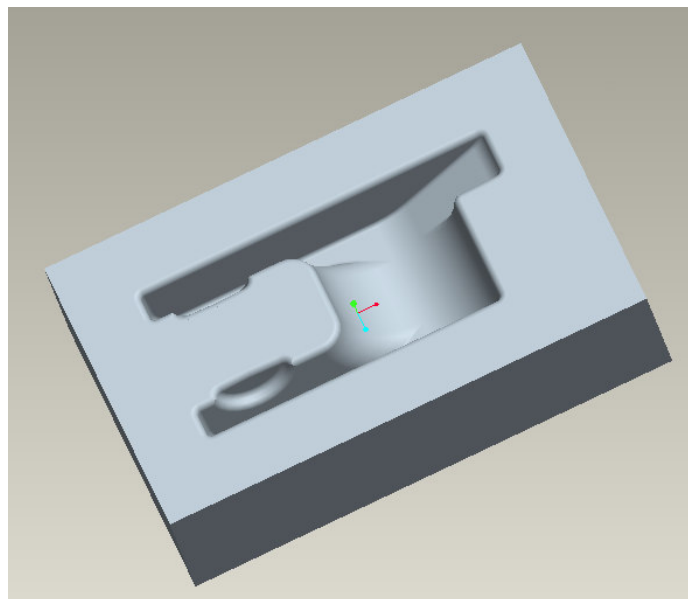


Fig. 3.6  Solid model of the lower die for final step of the forging.

### 3.3 Mesh Generation of the Parts

Elements have ideal shapes when there is little or no error in the numerical computation of individual stiffness matrices. It would be convenient if triangles were always equilateral, quadrilaterals always squares and hexahedra always cube. However, it is almost impossible to model complex systems with a mesh of ideally shaped elements. Therefore, it is advisable to match the mesh density to stress gradients and deformation patterns which imply that elements vary in size, have unequal side lengths and are warped or tapered. During mesh generation two matters must be consider during mesh generation; aspect ratio and distortions [44].

The element aspect ratio is the quotient between the longest and the shortest element dimensions. This ratio is by definition greater than or equal to one. If the aspect ratio (AR) is 1, the element is considered to be ideal with respect to this measure. Acceptable ranges for the aspect ratio are element and problem dependent, but a rule of thumb is:

AR < 3 for linear elements

AR < 10 for quadratic elements.

Elements with higher-order displacement functions and higher-order numerical quadrature for a given displacement function are less sensitive to large aspect ratios than linear elements. Elements in regions of material nonlinearities are more sensitive to changes in the aspect ratio than those in linear regions. If a problem has a deflection or stress gradient dominant in a single direction, elements may have relatively large (i.e.10) aspect ratios, provided that the shortest element dimension is in the direction of the maximum gradient.

Distortion is due to Skewing of elements and their out-of-plane warping is important considerations. Skewness is defined as the variation of element vertex angles from 90 degrees for quadrilaterals and from 60 degrees for triangles. Warping occurs when all the nodes of three-dimensional plates or shells do not lie on the same plane, or when the nodes on a single face of a

solid deviate from a single plane. In these cases contact penetration may occur because of distortion on the interface of contact bodies.

Using Finite Volume Method has an advantage that problems of mesh generation minimized in forging process simulation but in case of die analysis like die stress and die wear, it is important to create proper mesh for dies in order to obtain accurate results.

It is possible to import models from Pro/Engineer to MSC.SuperForge in STL or BDF formats, by means of these formats triangular meshes can be created on the surfaces of the parts. In this study, to create better mesh on the surfaces, mesh generation has been done in Pro/Engineer by using mechanical advanced mesh generation tool. The obtained mesh generation for the preform workpiece and the die are shown in figure 3.7 and 3.8, respectively.
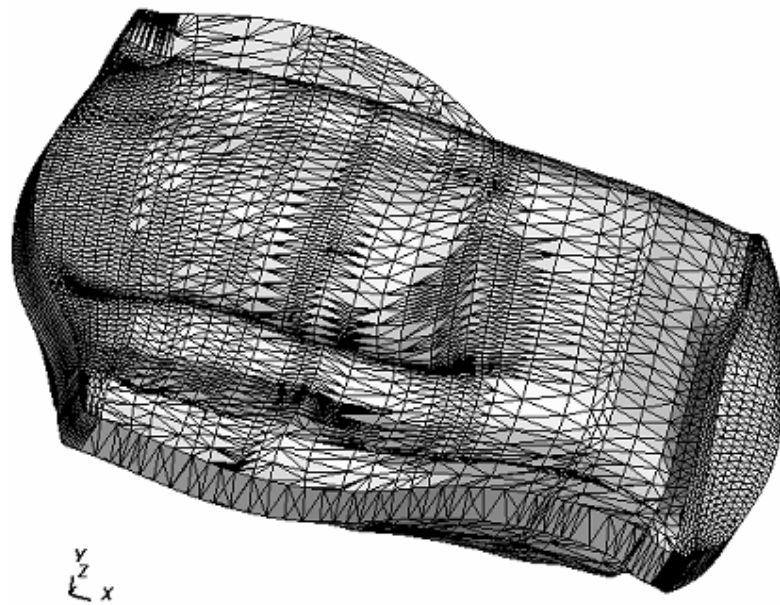


Fig. 3.7  Mesh generated in the preform workpiece.
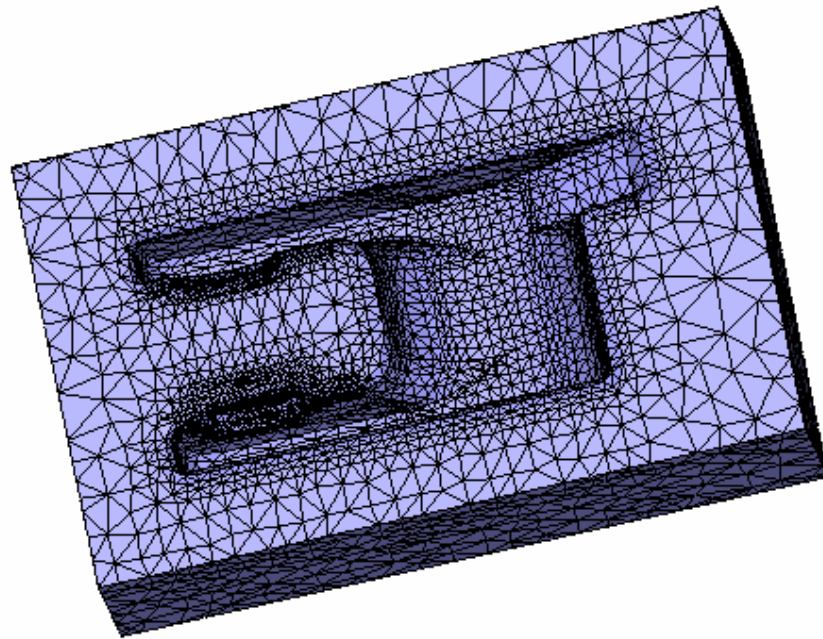
Fig. 3.8 Mesh generated using Pro/Engineer for the die .

# CHAPTER 4

# COMPUTER SIMULATION AND WEAR ANALYSIS
# OF HOT FORGING PROCESS

By knowing the value of wear coefficient for hot metal forming process, more accurate prediction can be done for die life during design of die. In this chapter, computer simulation of hot forging process has been done to obtain the wear depth of die, aim of this case study is to analyze the current forging process and comparing the result of wear analysis obtained from the computer simulation to the real-life experimental results. According to the analysis, a new wear coefficient for this case study which may be applied to the similar hot metal forming process will be suggested.

## 4.1 Analysis of Forging Operation Using Finite Volume  Method

In this study, as explained in chapter 1, MSC.SuperForge is used for the simulation and analysis. There are five common process parameters that are identical in all the simulations in order to obtain accurate results: workpiece and die models, material properties, ram speed, initial temperature, and friction model. After identifying those parameters, the simulation type and parameters must be assigned [18].

## 4.1.1 Importing Dies and Workpiece Models

The models for upper die, lower die and workpiece geometry should be imported to the program. It should be noted  that  MSC.SuperForge  requires a
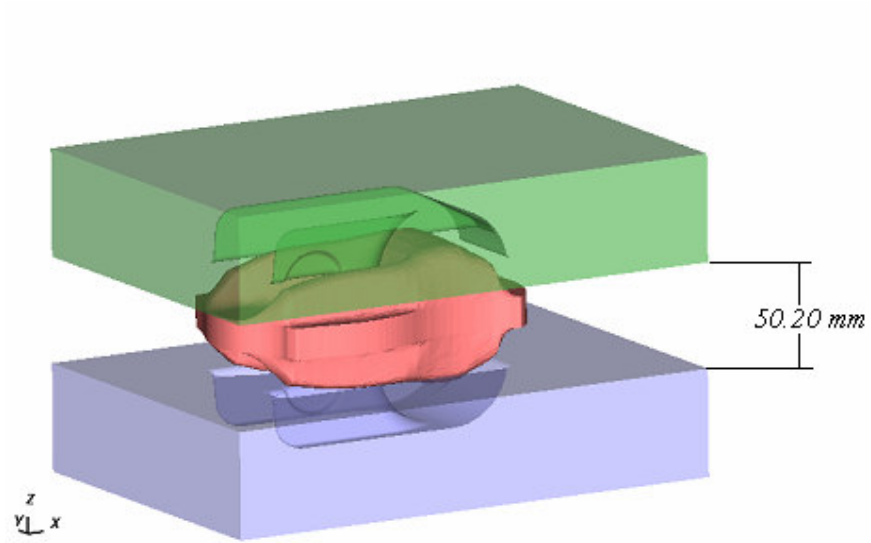
Fig. 4.1 Position of dies and workpiece in initial contact.

closed-volume surface model for both workpiece and dies. As explained in previous chapter, models should be imported to MSC.SuperForge in proper formats, BDF or STL, in these formats the surface models consist of triangular shaped facets only.

In MSC.SuperForge, forging operation direction is aligned on the Z axis, therefore after importing the models for the dies and the workpiece, the position of them with respect to each other and the forging direction may not be correct. These models are firstly aligned along the Z axis with using "Moving Option Toolbar". Once the objects are aligned along the Z axis, user can drop the workpiece in place and position the dies against the workpiece in initial contact by using "Positioning" option. The alignment of the dies and the workpiece and initial position of them is shown in figure 4.1.

### 4.1.2 Material Properties

There are the forging specific material models available for either cold forging or hot forging operations in the material library of the software. MSC.SuperForge provides elastic-plastic models for workpiece material, for

dies rigid-plastic models are used. In this study the workpiece material is X20Cr13 (DIN 1.4021), Heat Resisting Stainless steel. Figure 4.2 shows the workpiece stress-strain curve at a constant temperature of 1100$^{\circ}$C for three different strain rates [45].
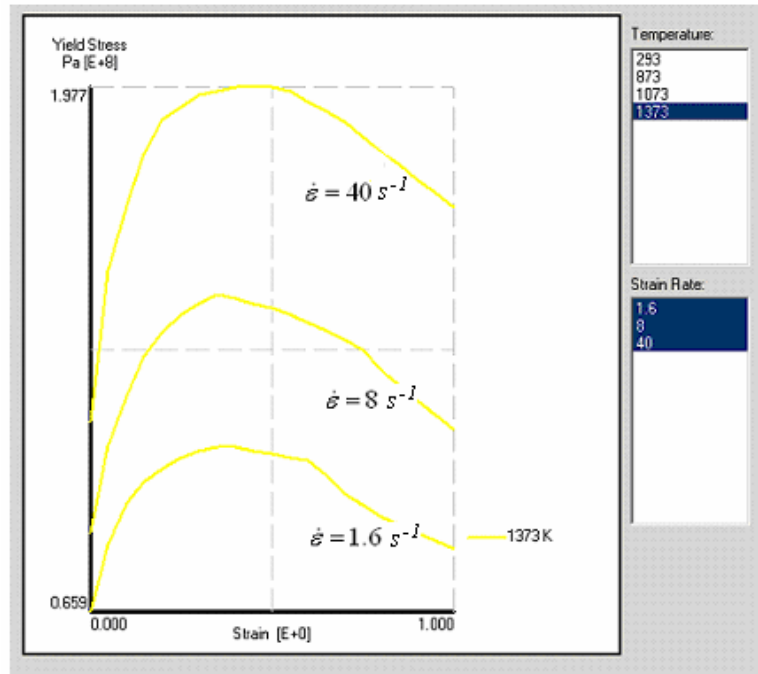


Fig. 4.2 Workpiece material stress-strain curve at 1100 $^{\circ}$C and different strain rates [45].

The die material is alloy tool steel AISI L6, Plasticity model for this material is as below [45]

$$\bar{\sigma} = \max[Y, C.\bar{\varepsilon}^{N}] \qquad (4.1)$$

where:

      $Y$ : Minimum Yield Stress: 645 MPa

      C : Yield Constant: 1.1735 GPa

      N : Strain Hard Exp.: 0.128

47

Figure 4.3 shows the plasticity behavior of die material used for simulation. The thermal properties and chemical compositions of the workpiece and the die materials are available in Appendix B.
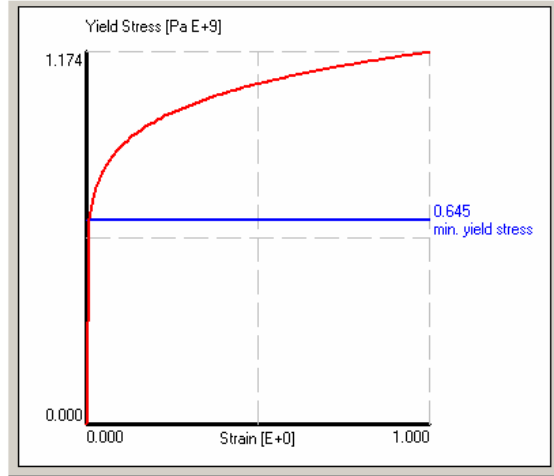


Fig. 4.3 Die material plastic behavior [45].

### 4.1.3 Forging Equipment

The software has six different types of forging machines that any of them can be applied for forging simulation; these are Crank press, Multi-blow Hammer, Screw Press, Hydraulic Press, Mechanical Press with Scotch Yoke drive and an alternate press defined by a table of time vs. speed. The Crank Press type, which is the forging machine used in AKSAN Forging Company, is used in this study, the required data is entered and these definition are assigned to the upper die. The entered data are given in Table 4.1.

Table 4.1. Properties of forging equipment

| Type of press | Mechanical Crank Press |
|---|---|
| Capacity of press | 1600 tonf |
| Crank Radius | 140 mm |
| Rod Length | 1000 mm |
| Crank Speed | 90 rpm |

By applying parameter given in Table 4.1 to the press, the velocity of the crank press can be obtained during its operation. Figure 4.4 shows the velocity of press as a function of time. At the beginning and at the end of press operation the velocity is zero. The maximum velocity of the press is 1.332 m/sec after 0.166 sec of press operation.
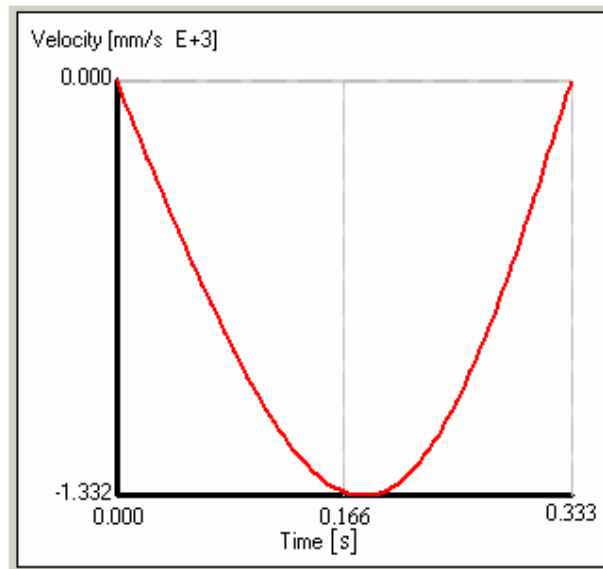


Fig. 4.4  The velocity of the crank press as a function of time.

**4.1.4 Initial Temperatures**

The initial temperatures of workpiece and dies have great effect on the simulation of hot forging process as they influence the plastic behavior of materials. In industry, the dies are generally preheated before using in hot forging process. The initial temperatures in this study are

Initial temperature of workpiece:          1100 $^{\circ}$C
Initial temperature of die:                300 $^{\circ}$C

Other parameters that used for the simulation are

Heat transfer coefficient to ambient: 50 watt/m$^2$.K

Heat transfer coefficient to workpiece: 6000 watt/m$^2$.K

Emissivity for heat radiation to ambient: 0.25

### 4.1.5 Friction Model

As the workpiece and the die have rough surfaces and are forced to move tangentially with respect to one another, frictional stresses will develop at the interface. Therefore, a friction model should be applied to both of the dies. For forging operations involving relatively low contact pressure between dry contact surfaces, the Coulomb's friction model is most appropriate [46]. If the frictional shear stress reaches a critical value, the workpiece will slip along the die. According to Coulomb's law of friction, this value is given by:

$$\tau = \mu \cdot \sigma_n \tag{4.2}$$

where, $\mu$ is the coefficient of friction and $\sigma_n$ denotes the normal stress at the workpiece-die interface.

The alternative model to Coulomb's law of friction is Tresca's friction model, which is the law of plastic shear friction. According to this model, if the frictional shear stress, $\tau$, exceeds a constant fraction $m$ of the flow stress in shear, $\tau_{yield}$, the workpiece starts to slip [46]:

$$\tau = m. \tau_{yield} \tag{4.3}$$

A value of zero represents perfect sliding, which means there is no shear or friction at the workpiece-die interface. A value of one represents sticking friction, which means that the friction shear stress equals the flow stress of the material in shear. For forging operations involving relatively high contact pressures, it is generally more appropriate to use the law of plastic shear friction [13, 46].

In this study, plastic shear friction model is used as friction model for the simulation. The coefficient of friction and the interface friction factor assumed as 0.3 and 0.05, respectively. These values were also used by other similar studies [25, 26, 27 and 28].

**4.1.6 Assigning Simulation Type and Parameters**

In this step, stroke of the operation, size of the finite volume workpiece and die element sizes, output step size (as percentage of the process time or in defined stroke step sizes), problem type (closed-die, open die, bending, forward extrusion, backward extrusion, rolling and also hot or cold forging) are defined. The suggested problem type for hot forging with flash by MSC.SuperForge is backward extrusion [47]. In this study this type of problem is selected. Also, a solver optimizer is implemented in this simulation control unit; thus, the user can change finite volume element size at any time and also coarsen the workpiece to decrease the number of elements. Parameters that are used in this stage are shown in Table 4.2 sample view of a completed simulation process can be seen in Figure 4.5.

Table 4.2 Operation parameters assigned to complete the simulation.

| Problem type | Hot forging-closed die with flash |
|---|---|
| Initial contact distance | 50.20 mm |
| Flash thickness | 6 mm |
| Upper die displacement | 44.20 mm |
| Workpiece element size | 2 mm |
| Die element size | 2 mm |
| Number of out put steps | 25 |
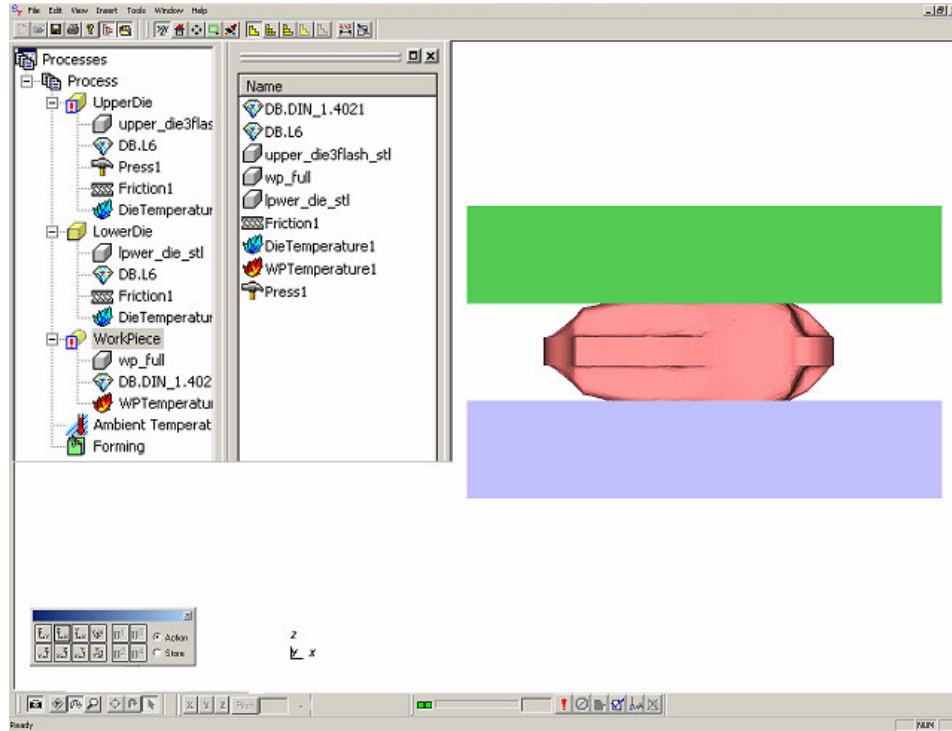
Fig. 4.5 Sample View of a Simulation Performed in MSC.SuperForge.

## 4.2 Wear Model Used in MSC.SuperForge

The wear model which is used in MSC.SuperForge is based on Archard's [34] wear model, offers depth of wear to be a function of sliding length, hardness, normal stress and wear coefficient. The relation is given by:

$$\Delta d = K \times \frac{P \times \Delta L}{H} \tag{4.4}$$

where:

$\Delta d$: depth of wear (mm) at each time increment $\Delta t$ (s),

$K$: non-dimensional wear coefficient,

$P$: contact pressure (Pa),

$\Delta L$: sliding distance (mm) at time increment $\Delta t$ and

$H$: hardness of die (Pa).

In Equation 4.4 the sliding distance can be replaced in term of sliding velocity, and value of $\frac{K}{H}$ can be replaced by dimensional wear coefficient $k$ Pa$^{-1}$.

$$\Delta L = U \times \Delta t \qquad (4.5)$$

$$k = \frac{K}{H} \qquad (4.6)$$

where:

$U$: sliding velocity (mm/s) at time increment $\Delta t$, and

$k$: dimensional wear coefficient (Pa$^{-1}$).

Equation 4.4 can be rephrased as:

$$\Delta d = k \times (P \cdot U \cdot \Delta t) \qquad (4.7)$$

To obtain final depth of wear for one cycle, Equation 4.7 can be written in summation form of each increment wear depth,

$$d_{fin} = \sum_{1}^{n} k \cdot P_i \cdot U_i \cdot \Delta t_i \qquad (4.8)$$

where:

$d_{fin}$ : Final wear depth at the end of one cycle,

$i$ : Number of increment,

$n$: Total number of increments that forging is simulated in one cycle.

The value of wear coefficient which is used in MSC.SuperForge to calculate the wear depth is $k = 1 \times 10^{-12}$ Pa$^{-1}$ [48]. Other parameters like contact pressure, sliding velocity, forging operation time and total number of increments will be calculated by numerical simulation.

## 4.3 Numerical Results of the Finite Volume Simulation

The Finite Volume simulation of this case study by using MSC.SuperForge took about 39 hours to complete one forging cycle. The operation time of forging, which is obtained from numerical studies, is equal to $8.74 \times 10^{-2}$ s, total increments for the simulation is 12675. The results can be

obtained in output increments which set to 25; therefore output time increment is $3.49 \times 10^{-3}$ s. Figure 4.6 shows the preform workpiece at the beginning of simulation and final production result of the forging simulation.
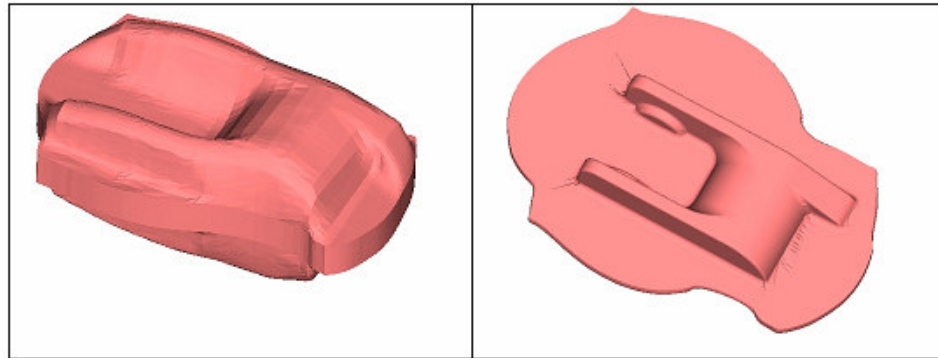


Fig.4.6  Preform work piece (Left), result of simulation- final production (Right).

In addition to obtaining depth of wear from numerical result, other parameters like contact pressure, sliding velocity, effective stress, surface temperature and workpiece-die contact will be used to analyze wear generation on the die surface. In Figure 4.7 the velocity of the upper die is shown during the forging operation. At t = 0, beginning of the forging operation, the workpiece and the upper die are in initial contact. At this moment the velocity of the upper die is about 1 m/sec. At t = 0.087 s  the upper die reaches to its maximum displacement and the forging process will be completed.
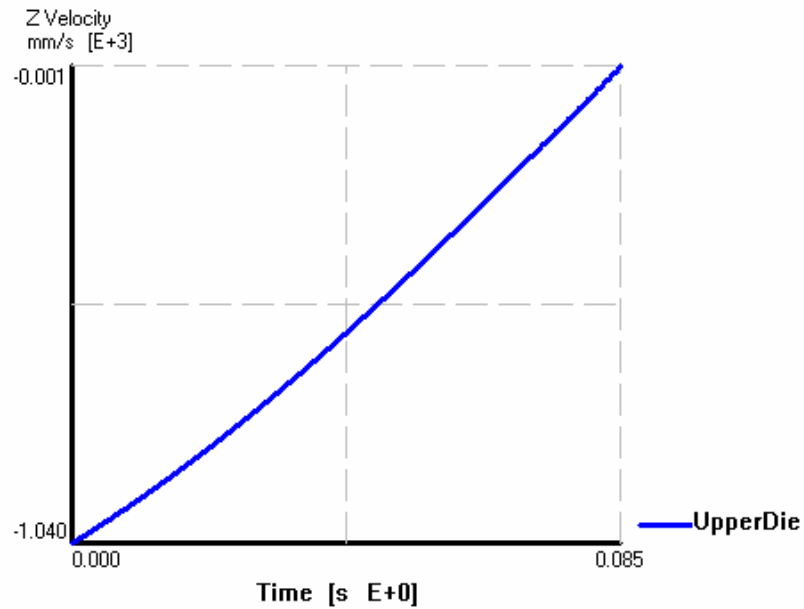
Fig. 4.7 The velocity of the upper die as a function of operation time.

## 4.4 Wear Analysis of the Die

Wear analysis has been done by comparing numerical result of die wear from the forging simulation with the measurement of the worn die by using Coordinate Measuring Machine (CMM).

From studying the result of die wear from simulation results, it will be understood that depth of wear is larger on the round edges and thin sections of die where depth of wear may reaches to $9\times10^{-3}$ mm in the first forging operation, which is a large value of wear and this much depth of wear will reduce the die life so much. On the base plane of cavity depth of wear is very small, about $0.05\times10^{-3}$ which can be neglected due to no affect on die life. In Figure 4.8, four areas with large depth of wear which obtained from numerical analysis are shown. There will be a study in each region by choosing a certain cross section (CAD Profile) and comparing numerical results (Wear Analysis Profile) with same cross section from measurement of worn die by CMM.
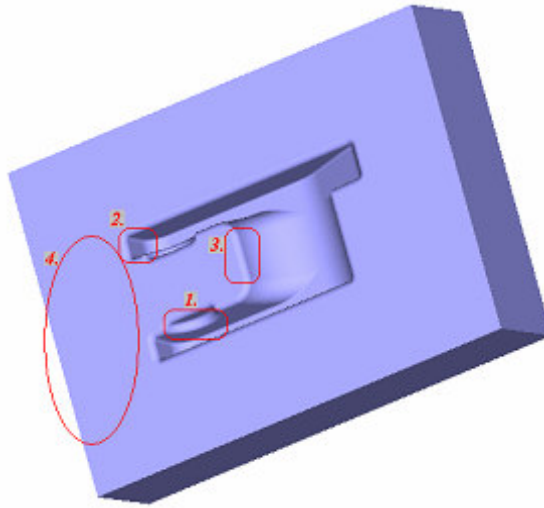
Fig. 4.8 Four areas with high depth of wear which obtained from numerical analysis.

### 4.4.1 Wear Analysis of the Die in Region 1

Figure 4.9 shows the certain cross section in region 1, that the result of wear analysis will be discussed. The original die profile form CAD data and the worn die profile measured by CMM is shown in Figure 4.10 on one half of the profile. Since wear is result of surfaces contact, and surfaces contact has great effect on amount of wear, the process of the die filling in the selected cross section is given in Figure 4.11 at different stages of the simulation of forging operation.
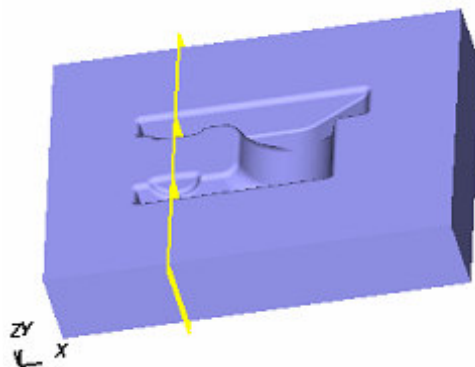


Fig. 4.9  Section 1 of the die.
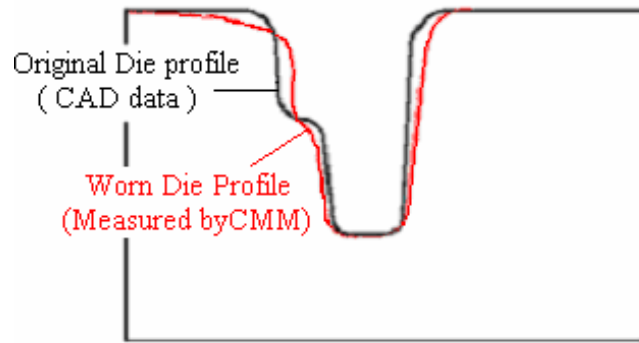
Fig. 4.10 Comparing the original die profile with the
worn die profile measured by CMM in section 1.

The results of wear depth that obtained from simulation show that this value is large on the parting line and close to that, the maximum value reaches to $3.2\times10^{-3}$ mm at parting line and the minimum depth of wear is about $4\times10^{-5}$ mm at the middle of the wear profile in the corner. This area is one of the last spots to be filled during the process (Figure 4.11.d), also due to the same reason at the base line of profile there is small value of wear depth which is $0.24\times10^{-3}$ mm.



*a) 0%*          *b) 32%*          *c) 48%*          *d) 72%*
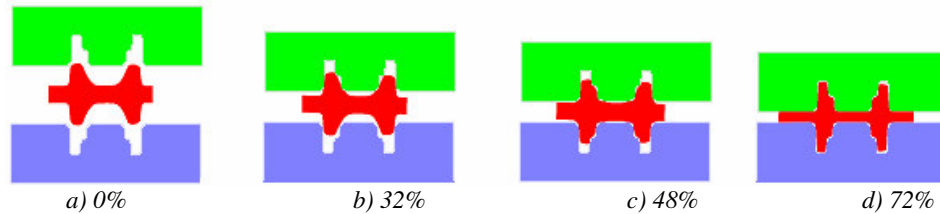
Fig. 4.11 Die filling in section 1in different time stages of the forging
simulation (in percentage of the operation time of forging).

Figure 4.12 shows the value of wear depth at the end of the first cycle forging operation simulation. Values in parentheses shows wear depth after batch size of 678. By using these values it is possible to draw wear profile and compare the numerical results with the measured values on the worn die

57

(Figure 4.13). By comparing the wear analysis results and the worn die measurement results with the original die profile (Figure 4.13), it can be understood that there is a plastic deformation on the upper part of profile. This plastic deformation of the die can be due to flash formation between upper and lower dies which cause high effective stress. It seems for better study of the wear analysis; the plastic deformation of the die must be mentioned in this study.
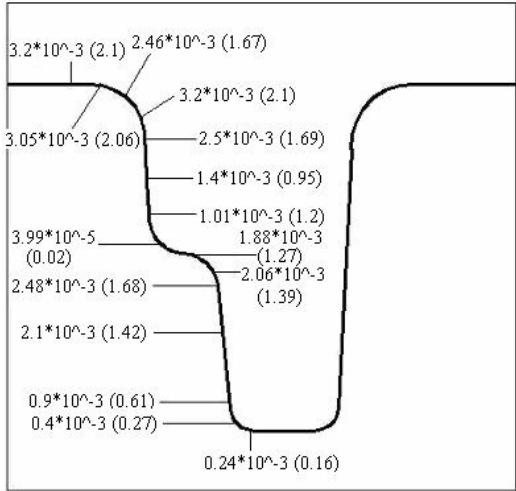


Fig. 4.12 Wear depth (mm) for k $=1\times10^{-12}$ Pa$^{-1}$ in one cycle of forging in section 1. (Values in parenthesis show wear depth of a batch).
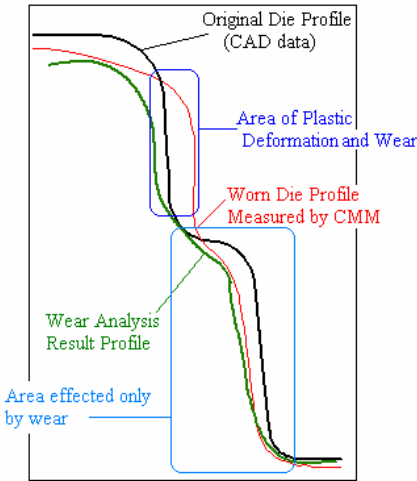


Fig. 4.13 Comparison of wear analysis result and the worn die measurement by CMM in section 1.

On the lower area of the wear profile, there is a fair agreement between the wear profile and CMM measurement profile. It shows that there is no plastic deformation in this part of the die and the change in profile is mainly due to wear. But in some part, there is relatively large difference, since in simulation process dimensional wear coefficient is taken as $10^{-12}$ Pa$^{-1}$, it can be understood that some evaluation is needed for wear coefficient to get better results compare to the worn die measured results.

### 4.4.1.1 Plastic Deformation of the Die

Plastic deformation in die occurs due to high stresses occurring during metal forming process. The mechanical press load-time graph is shown in Figure 4.14. In this mechanical crank press, the maximum force appears at 88% of operation cycle with value of 4949 kN. Therefore, the highest stress must occur in this range of operation.

By studying the die stress analysis, the maximum value of effective stress can be obtained. As expected, the highest stresses appear when the force is at its maximum value.
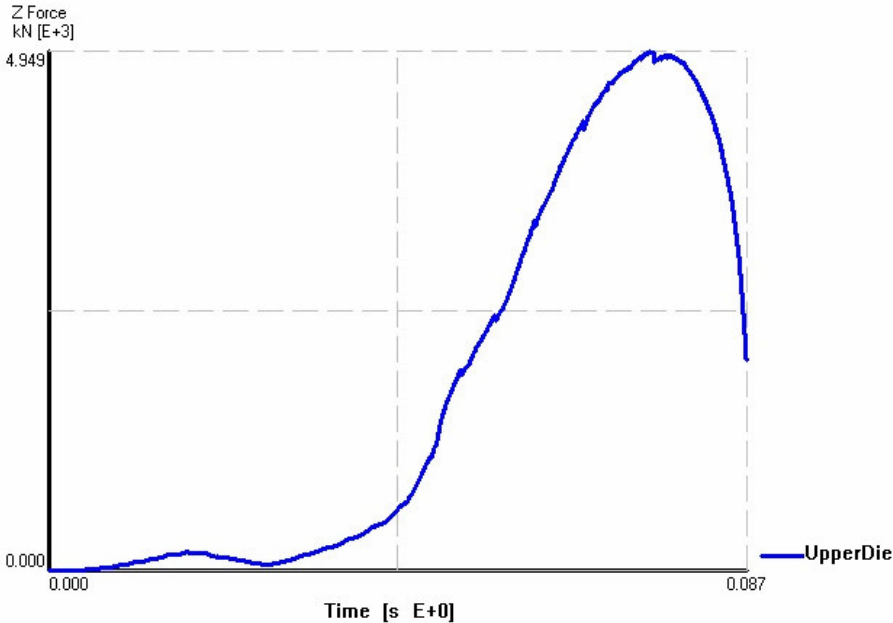


Fig. 4.14 Forging Load as function of operation time.

As explained in the material properties part, Section 4.1.2, the plastic behavior of the die material is assumed to be rigid-plastic and the stress-strain diagram is shown in Figure 4.3, with the minimum yield stress of 645 MPa. In the deformation analysis of die, on the nodes where the effective stress is above 645 MPa, the plastic deformation is assumed to appear otherwise there is no plastic deformation. The highest values of effective stresses are shown in Figure 4.15. On the upper part of profile effective stresses exceed the rigid limit and in greatest value it is about 780 MPa, but in the lower part of the profile effective stresses hardly pass 400 MPa, then in this part only wear would cause deformation and no plastic deformation on the die exists.

Figure 4.16 shows the plastic deformation of die profile; which is obtained from the finite volume analysis, compare to the original die profile and the worn die profile. The maximum plastic deformation is equal to 3.71 mm that appears in the forging simulation.
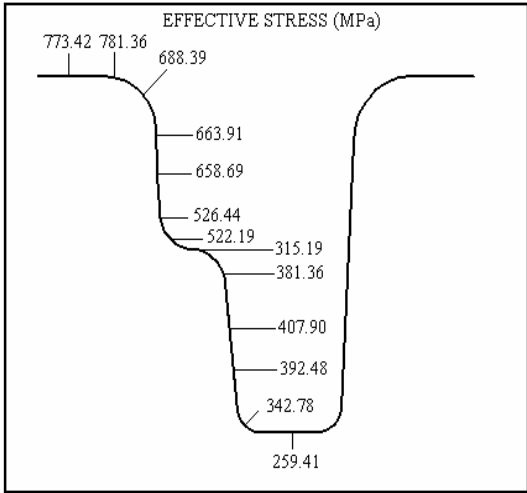


Fig. 4.15 The maximum effective stresses MPa,
that appears at 80% of operation time in section 1.

.
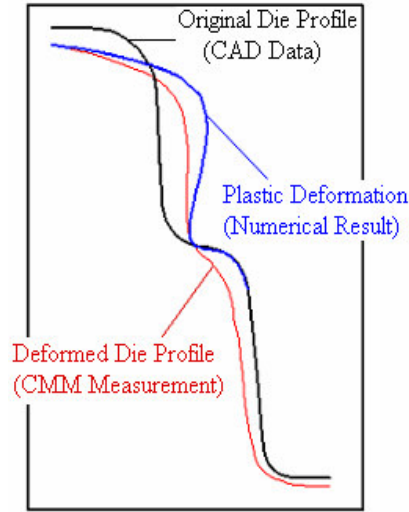
Fig. 4.16 Plastic deformation from Result of FV analysis in Section 1.

### 4.4.1.2 Evaluation of Wear Coefficient by Using Worn Die Measurement

From comparison of wear analysis profile and measured worn die profile in Figure 4.13, it can be understood that there are some disagreements between these two. These differences explain the need of modification in wear coefficient which is taken as $1\times10^{-12}$ Pa$^{-1}$ in die wear analysis of MSC.SuperForge.

The aim of using finite volume method in wear analysis is to obtain contact stress and sliding velocity fields to use in proper wear model. These fields of contact stress and sliding velocity can be obtained from numerical results; the wear model used for numerical analysis is in form of

$$d_{fin} = \sum_{1}^{n} k \cdot P_i \cdot U_i \cdot \Delta t_i \tag{4.9}$$

where, $d_{fin}$ is known from numerical results and $k$ has constant value $10^{-12}$, by knowing these values, $\sum_{1}^{n}(P_i \cdot U_i \cdot \Delta t_i)$ will be calculated,

$$\sum_{1}^{n}(P_i \cdot U_i \cdot \Delta t_i) = \frac{d_{fin}}{10^{-12}} \tag{4.10}$$

61

By knowing $\sum_1^n (P_i \cdot U_i \cdot \Delta t_i)$ and $d_{true}$ (the true value of wear depth, measured from worn die) new value of $k$ can be calculated for each point.

$$k = \frac{d_{true}}{\sum_1^n (P_i \cdot U_i \cdot \Delta t_i)} \qquad (4.11)$$

In Figure 4.17 evaluated dimensional wear coefficient in different points are shown, it changes from $5.7 \times 10^{-13}$ (about half of initial value of $k$) to $9.25 \times 10^{-13}$ (nearly equal to initial value of $k$). The average wear coefficient were evaluated for these points, that is $k = 7.48 \times 10^{-13}$.
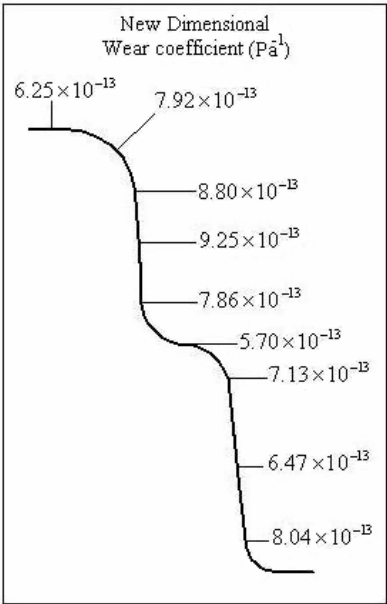


Fig. 4.17 Dimensional wear coefficients evaluated
for different points in section 1.

wear analysis will be done by using the evaluated value of $k$, and new profile will be obtain considering both wear and plastic deformation (Figure 4.18). Comparison between the profile of actual deformed die profile (measured by CMM) and that of calculation show very similar results. It means the new wear coefficient is a good approximation for die wear analysis.
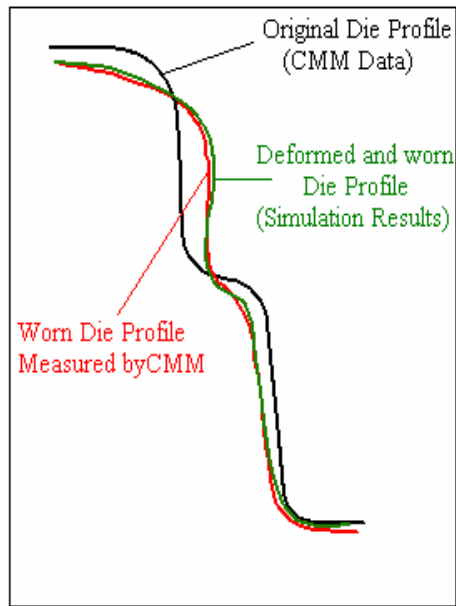
Fig. 4.18 Comparison between deformed die profile
for $k=7.48\times10^{-13}Pa^{-1}$ and worn die measurement
by CMM in section 1.

### 4.4.1.3 Parameters Affecting Wear Analysis

In addition to effect of wear coefficient in wear analysis other parameters like contact pressure, sliding distance, contact time between die and workpiece, and temperature increase on the surface of the die have great effect on die analysis.

Since wear is result of contact between surfaces, the contact pressure and sliding distance have great effect on wear depth. It is obvious that these parameters have meaning when contact happens between workpiece and die surface. Then for wear analysis, it is important to study the time that different points of die are in contact with workpiece. Therefore, even some points have high value of contact pressure and sliding length, but there is a small value of wear. In this case, time of contact must be studied. For example some point are in contact from the beginning to the end of operation (100% of operation time), and there are some points, like thin rips, that they come to contact few percentage of operation time, say 20%, then amount of wear would be much

higher in first point than second point even during contact there are higher contact pressure or sliding length at second point. Figure 4.19 shows the process of contact between workpiece and die, and Figures 4.20 and 4.21 show the maximum contact pressure and the maximum velocity during operation and values in parenthesis, in Figure 4.21, show the percentage of operation time that those points of the die are in contact with the workpiece.
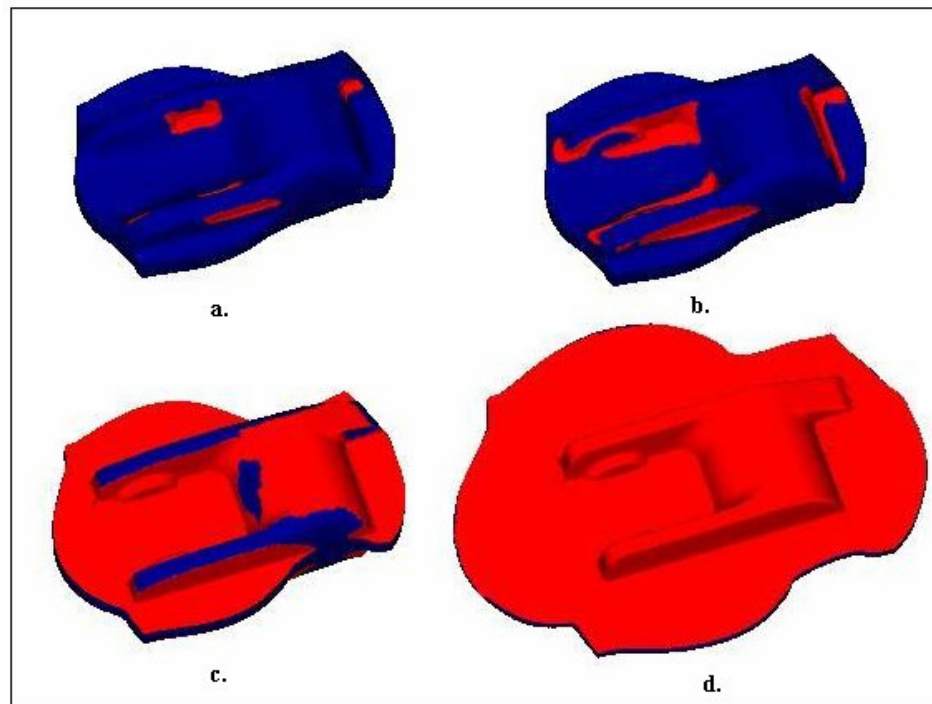


Fig. 4.19 Contact between die and workpiece in different stages. Red color shows contact between die and workpiece. a) after 12% progress in operation, b)25%, c)65% and d)100%.

The other important parameter that affects wear is the surface temperature of the die. In hot forging process, a high temperature billet is in contact with the die relatively at lower temperature. Due to large temperature differences, there will be rapid change in the temperature of die. This change of temperature is cause of two main factors: friction on the contact interface and heat transfer
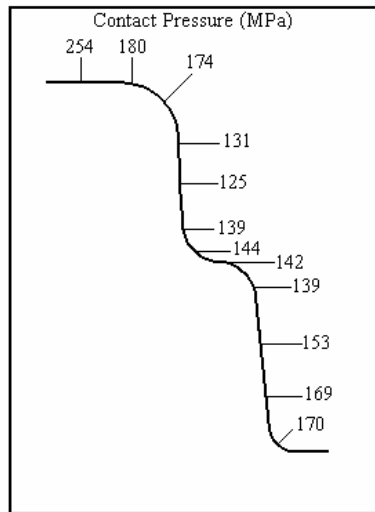
Fig. 4.20 The maximum contact pressure MPa, during forging operation that appears at different time steps in section 1.
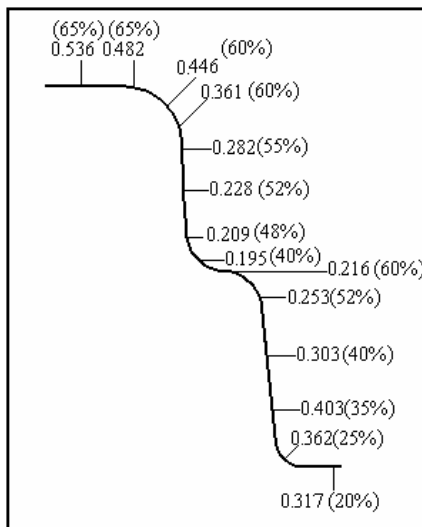


Fig.4.21. Maximum sliding velocities (m/s), and percentage of total contact periods in parenthesis at different points in section 1.

from hot workpiece to the die. Friction can be reduced by using proper lubrication after each cycle. By making the operation time as small as possible, the heat transfer can be reduced so much. By increasing the temperature of die, the wear coefficient increases so much some times up to 150% [42] and the hardness of die decreases by increasing of temperature (See

65

Appendix B). Then amount of wear may increase sharply by raising temperature on the surface of die.

The final surface temperature of the die can be obtained from the simulation of hot forging process. In this case study, the highest temperature is about to 370 $^\circ$C (Figure 4.22). Since the initial temperature of die is 300 $^\circ$C, there is no large increase in the die temperature. That could be due to small operation time (i.e. $8.74 \times 10^{-2}$ s), then the hardness of die and wear coefficient do not change during the process. Therefore, assuming constant dimensional wear coefficient is a good approximation for this analysis.
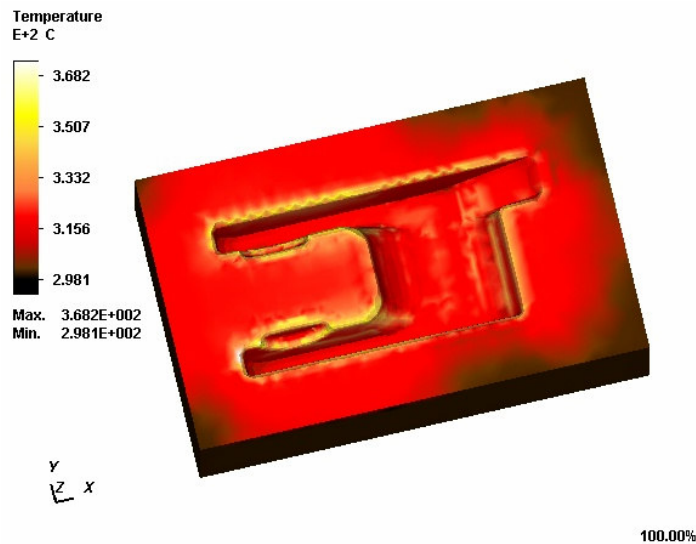


Fig. 4.22  Temperature distribution of the die at the end of process time.

### 4.4.2 Wear Analysis of Regions 2 and 3

In this section, two other cross sections in regions 2 and 3 will be selected for analysis in the same way as done in the previous sections. New value of dimensional wear coefficient will be evaluated and by using this new value a modified wear profile will be compared with the measured worn die

profile. Figure 4.23 shows the cross section which is chosen to study in region 2; it is located in thin section of cavity and close to flash land (region 2 in Figure 4.8). The original die profile and the measured worn die profile are shown in Figure 4.24. The comparison of these two profiles shows the largest depth of wear about 2.5 mm near the parting line. Filling of the die in selected cross section in different percentage of forging process time is shown in Figure 4.25.
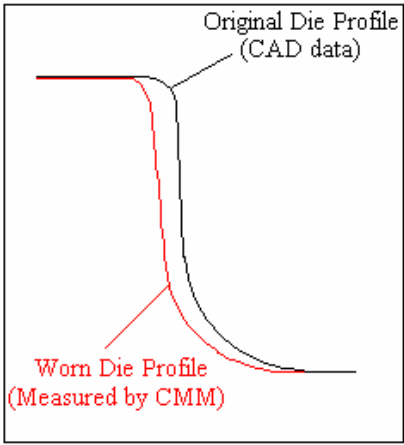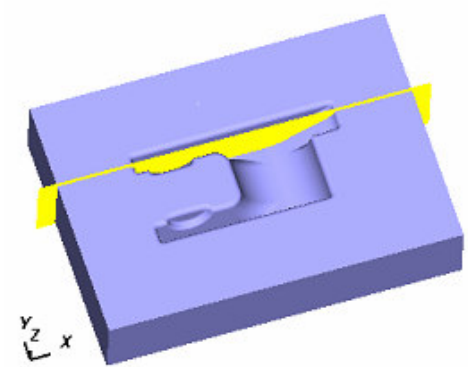


Fig. 4.23 Section 2 of the die.     Fig. 4.24 Comparing the original die profile with the worn die profile measured by CMM in section 2.



*a) 0%*          *b) 36%*          *c) 64%*          *d) 100%*
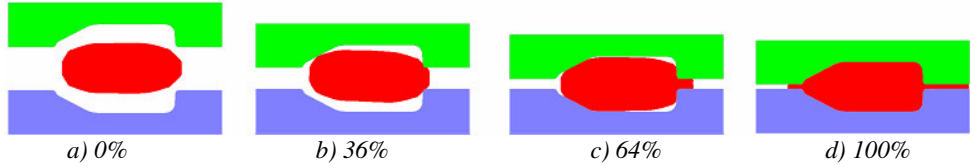
Fig. 4.25 Die filling process in cross section 2. in different time stages (in percentage) of the forging simulation.

The results of wear depth analysis that obtained from forging simulation by Finite Volume Method show that the maximum value reaches to $7.5 \times 10^{-3}$ mm close to the parting line. The minimum depth of wear is about $5 \times 10^{-5}$ mm at the bottom line of the die profile, this area is one of the last spots to be filled during the forging process with small contact time, therefore

the amount of wear is very small due to small contact time, as shown in Figure 4.25 after 64% progress of the forging operation time this point would come into contact with workpiece.

The values of wear depth at the end of the first forging operation cycle simulation are shown in Figure 4.26. The values in parentheses show the wear depth after batch size of 678. By using these values it is possible to draw wear profile and compare the numerical results with the measurement of the worn die. Figure 4.27 shows the comparison of CAD data, the CMM measurement and the wear analysis results.
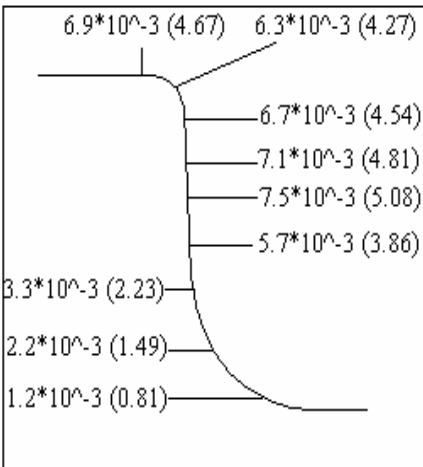


Fig. 4.26 Wear depth (mm) for $k = 1 \times 10^{-12} \ Pa^{-1}$ in one cycle, in section 2. (Values in parenthesis show wear depth after batch size of 678,).
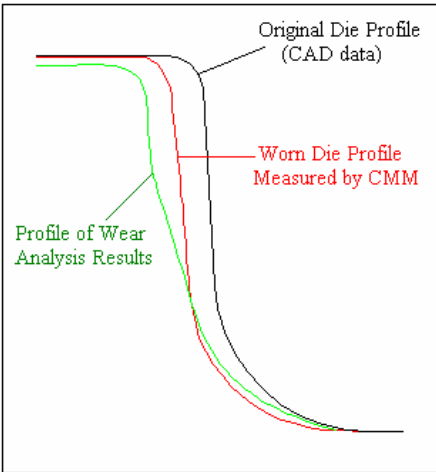


Fig. 4.27 Comparison of wear analysis result and the worn die measurement by CMM in section 2.

By comparing the result of wear analysis profile form forging operation simulation with the worn die profile measured by CMM, it can be understood that there is a fair agreement between profiles. To obtain better results there should be some evaluation on wear coefficient in order to get acceptable results compare to measured worn die profile. Same way as explained in the previous sections will be used to evaluate new dimensional wear coefficient. New values of wear coefficient at different points are shown in Figure 4.28. The largest value is $8.75 \times 10^{-13}$ at the middle of the profile and the smallest is equal to $0.11 \times 10^{-13}$ at the bottom line of the profile. Values of wear coefficient are about $5 \times 10^{-13}$ close to the parting line. The average value of dimensional wear coefficient in different points is equal to $6.75 \times 10^{-13}$. By using this average value of the wear coefficient it is possible to calculate new depth of wear at points and new profile can be obtained, this new profile is shown in Figure 4.29. The maximum contact pressures attained during the forging simulation at different points of the die are shown in Figure 4.30. The maximum sliding velocities attained during the forging simulation are shown in Figure 4.31. Values in parentheses in Figure 4.31 show the percentage of operation time that those points of the die are in contact with the workpiece.
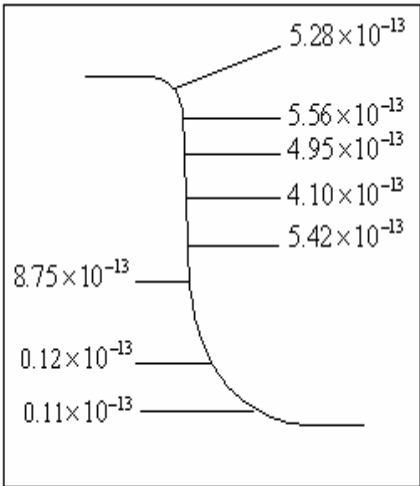


Fig. 4.28 Dimensional wear coefficients $k$ Pa$^{-1}$ evaluated for different points in section 2.
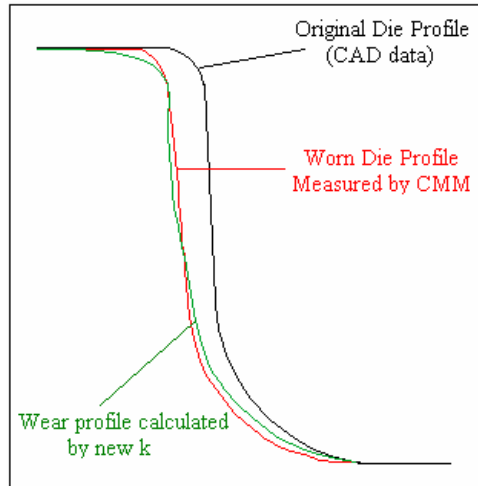
Fig. 4.29 Comparison between wear profile calculated for $k=6.75\times10^{-13}$Pa$^{-1}$ and profile measured from the worn die in section 2.
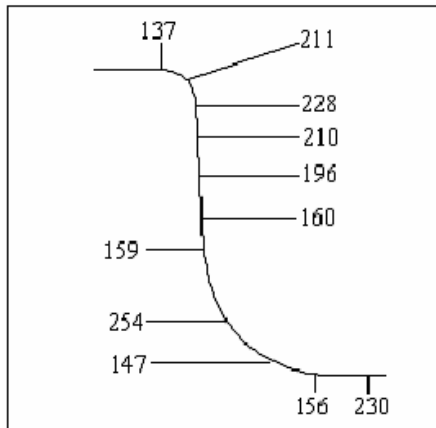


Fig. 4.30. The maximum contact pressure MPa, attained during the simulation in section 2.
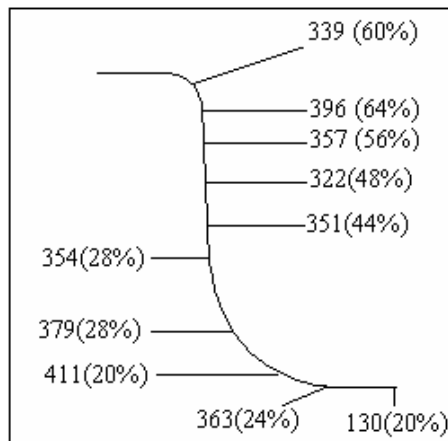


Fig.4.31. Maximum sliding velocities (mm/s),and percentage of total contact periods in parenthesis for different points in section 2.

70

Other cross section at region 3 has been selected and wear analysis of this certain section has done. The selected cross section from die is shown in Figure 4.32 and the original die profile from CAD data and the worn die profile measured by CMM, are shown in Figure 4.33. The process of die filling in selected cross section is showed at different stages of forging operation time in Figure 4.34.
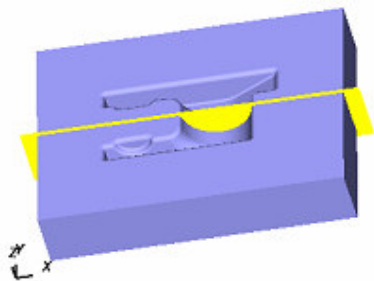


Fig. 4.32 Section 3 of the die.
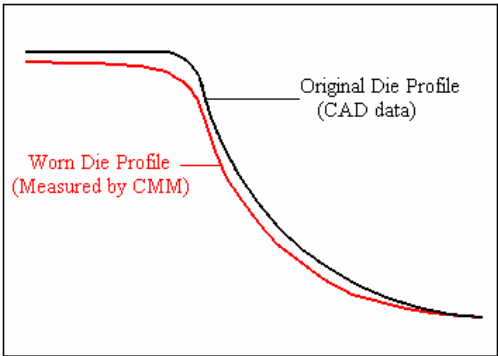
Fig. 4.33 Comparing the original die profile with the worn die profile measured by CMM in section 3.



a) 0%          b) 40%          c) 52%          d) 100%
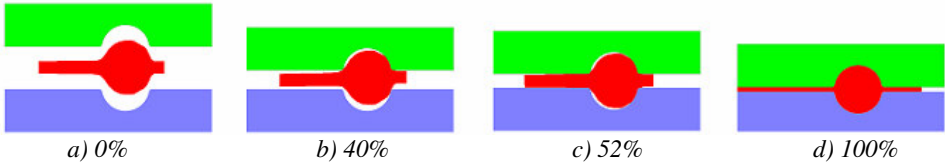
Fig. 4.34 Die filling in cross-section 3 in different time stages (in percentage) of the  forging simulation.

The results of wear depth that are obtained from the forging simulation show that the largest value of wear depth appears at the round curve at the top of the profile and it is equal to $7.3 \times 10^{-3}$ mm. At the lower part of the profile the value of wear depth is small and at the lowest point it is almost zero.

Figure 4.35 shows the values of wear depth at the end of one cycle forging operation simulation with $k = 1 \times 10^{-12}$. The values in parentheses show the wear depth after batch size of 678. By using these values from numerical simulation wear profile at this cross section will be compared with the measurement of worn die (Figure 4.36).
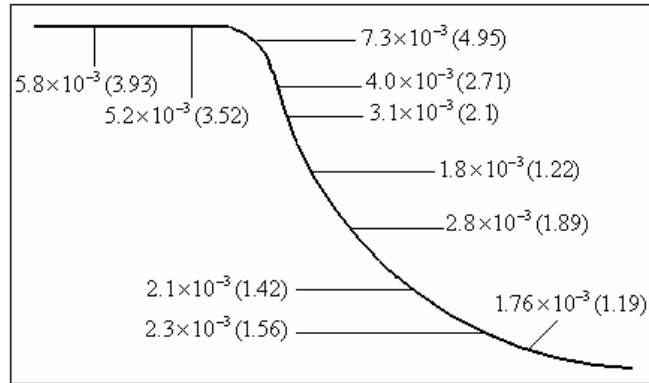


Fig. 4.35 Wear depth (mm) for $k = 1 \times 10^{-12} \, Pa^{-1}$ in one cycle in Section3. (Values in parenthesis show wear depth after batch size of 678).
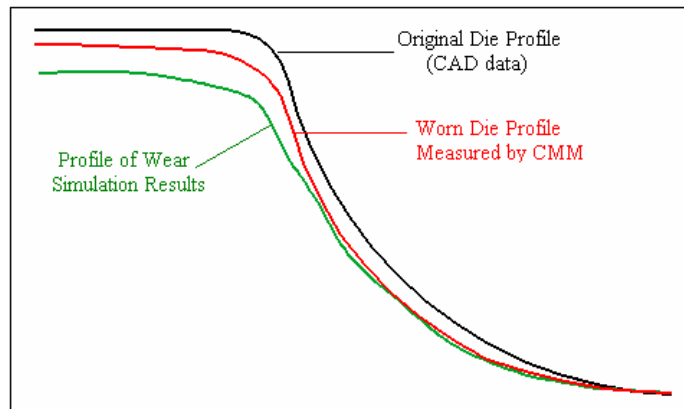


Fig. 4.36 Comparison of wear analysis result for $k = 1 \times 10^{-12} \, Pa^{-1}$ with the worn die profile measured by CMM in section 3.

By obtaining forging simulation results, evaluation must be done on wear coefficient. Figure 4.37 shows the evaluated wear coefficient in different points. The largest value is *9.25×10$^{-13}$* and the smallest is equal to *2.93×10$^{-13}$*.
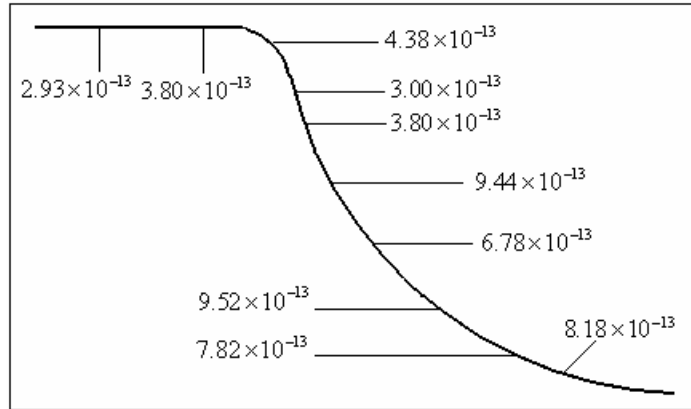


Fig. 4.37 Dimensional wear coefficients $k$ Pa$^{-1}$ evaluated at different points in section 3.

By using these evaluated wear coefficients in different points an approximate value will be calculated, the value is $k=$ *5.96×10$^{-13}$*. By using this evaluated value a new wear profile can be obtained (Figure 4.38). The new value of $k$ is a good approximation compare to the measured worn die profile. Contact pressures and sliding velocities are shown in Figure 4.39 and 4.40, respectively.
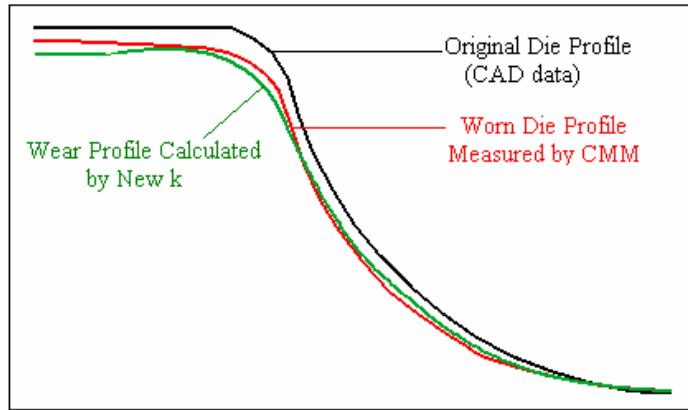
Fig. 4.38 Comparison between wear profile calculated by k=5.96×10$^{-13}$Pa$^{-1}$ and worn die profile measurement by CMM in section 3.
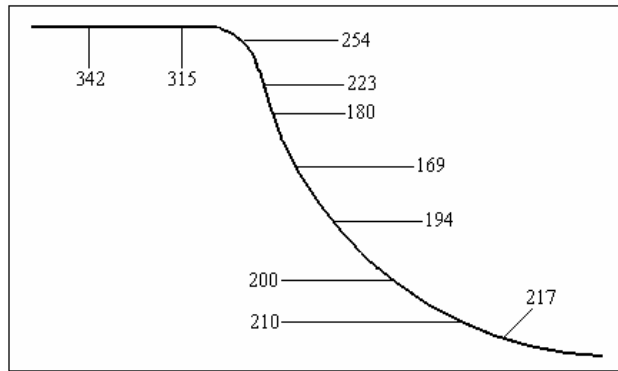


Fig. 4.39 The maximum contact pressure (MPa) at different points in section 3.
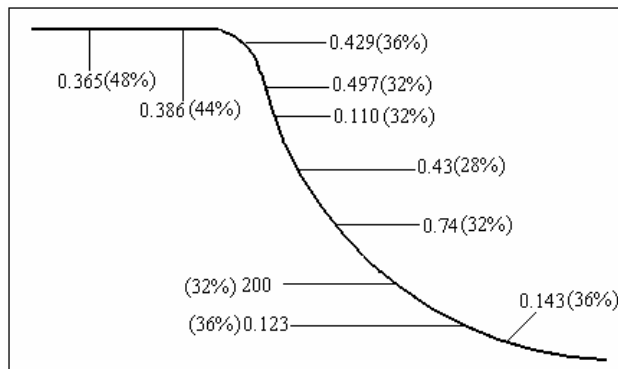


Fig. 4.40 Maximum sliding velocities (m/s) at different points in section 3, and percentage of total contact periods (in parenthesis).

74

### 4.4.3 Wear Analysis on the Flash Land of the Die

Result of wear analysis for forging process shows relatively high depth of wear in flash land (region 4 in Figure 4.8), it reaches to 0.2 mm at the end of first forging cycle. This large value of wear depth is due to large contact pressure and sliding velocity, as contact pressure in its maximum is 300 MPa (Figure 4.41) and sliding velocity reaches to 1.7 m/s (Fig. 4.42). Studying the worn die shows that the real-life value of wear depth is much smaller than simulation analysis results. This difference would be cause of change of wear mechanism from mechanical wear regime to oxidation wear regime.

Oxidational wear appears when steel surfaces slide at velocities above 1 m/s [25], this velocity is just sufficient to give flash temperatures which will cause oxidation (see Section 2.2.3). Now by using Equation 2.11, a new value of wear depth will be calculated. The average values of contact pressures and sliding velocities will be used in Equation 2.11, $P_{ave}$ = 150 MPa and $U_{ave}$ = 1.2 m/s, flash formation starts after 50% of operation, therefore contact time should be mention half of total operation time. To obtain non-dimensional pressure, the hardness of the die is assumed as 1.5 GPa. Then for wear calculation the normalized parameters are $\tilde{P} = 0.1$ and $\tilde{U} = 158$. Value
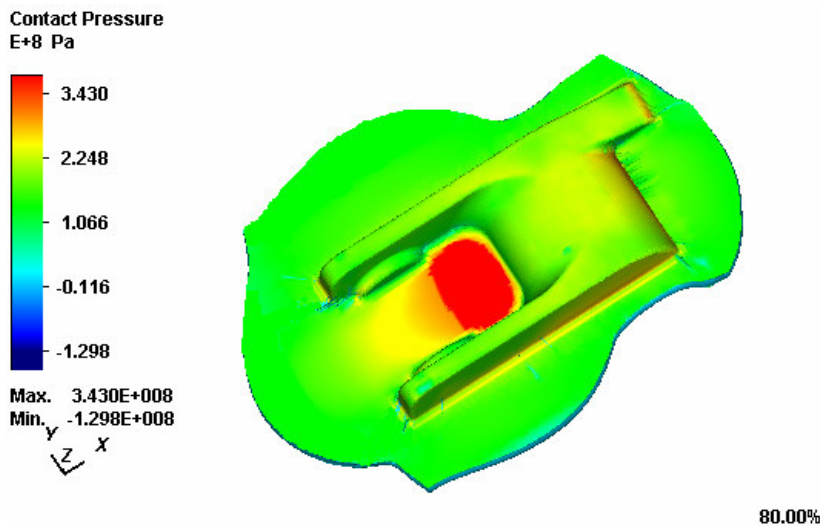


Fig. 4.41 The Maximum contact pressure appears after 80% of operation progress time.
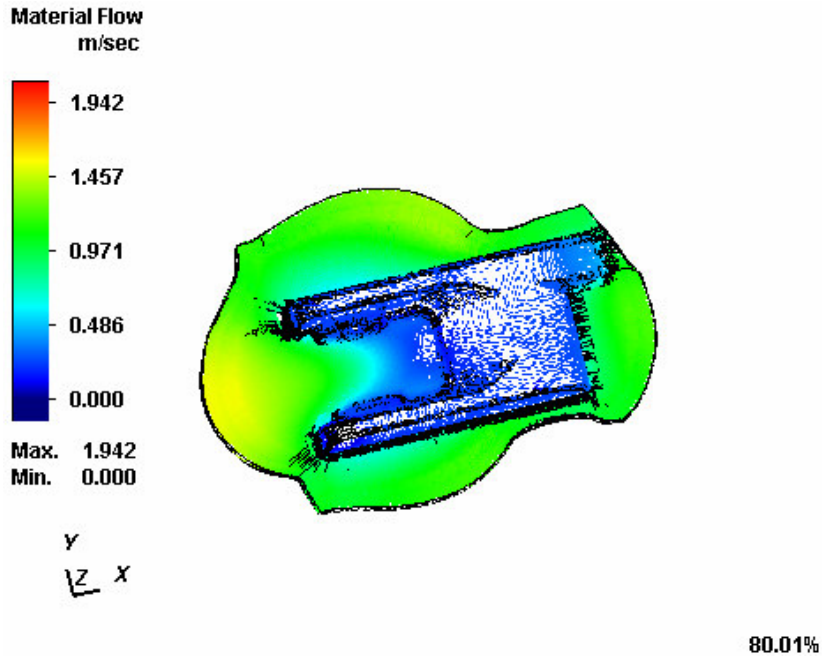
Fig. 4.42 The sliding velocity at 80% of operation time.

of $1.04 \times 10^{-3}$ will obtain for wear depth for one cycle of forging, after batch size of 678, the depth of wear will be 0.70 mm, which is in better agreement than mechanical wear model with experimental results.

By using the result of wear depth calculated by oxidational wear mechanism, it is possible to obtain a non-dimensional wear coefficient for this condition by using Equation 4.11.

$$0.7(mm) = k \times \{150 \times 10^6 (Pa) \cdot 1200(mm/s) \cdot 8.74 \times 10^{-2}(s) \times 0.50\}$$

The value obtained from above is $k = 1.32 \times 10^{-13}$ (Pa$^{-1}$), as expected this value is much smaller than wear coefficients of mechanical wear models. This value is also in agreement with wear map, as in wear map, the contour of normalized wear decrease by entering the oxidational wear regime.

# CHAPTER 5

# DISCUSSION AND CONCLUSION

## 5.1 Discussion of the Results

In this thesis study, the wear analysis has been done for a hot forging finishing die, provided by AKSAN Forging Company [8]. Finite Volume Method was used to simulate the hot forging process. The die wear option of MSC.SuperForge was used to obtain wear depth of the die. The parameters affecting the wear like contact pressure, sliding velocities, plastic deformation, surface temperature and etc, were obtained from numerical results of the forging simulation.

The mechanical press with capacity of 1600 tons was used for the forging. During the forging operation, after 84% of the operation time (i.e. $t = 7.3 \times 10^{-2}$), the maximum force reaches to about 5000 kN. About this time of operation, the effective stresses reach to their maximum value in the die through the forging process. The maximum effective stress is close to 800 MPa. By reaching to this value, plastic deformation occurs in the die due to high effective stress and also fatigue due to the repetitive forging processes in a batch. Both wear and the plastic deformation of the die would be studied at the points of the die with high effective stress.

The highest value of normal contact pressure appears at about 80% of the operation time on the top flat surface of the die with a value of 343 MPa. The contact pressure is about 200 MPa on the round corners. On the flash land, the normal contact pressure is about 150 MPa. The maximum sliding velocity occurs in flash land, reaches to about 1.6 m/sec. In the cavity, the sliding velocity is about 0.5 m/sec and in narrow sections it is about 0.3 m/sec which are much smaller than the sliding velocity in the flash land.

For the wear analysis, the flash land and three different sections, where large depth of wear was observed, were chosen and the wear coefficients in these sections were evaluated. In this study, dimensional wear coefficient $k$ (i.e. $\frac{K}{H}$) was used for the simulation. Using of the dimensional wear coefficient has advantages due to the fact that the changes of the non-dimensional wear coefficient and hardness of the die would be taken to account at the same time as one parameter.

It has been observed that by using constant initial value of dimensional wear coefficient of $10^{-12}$ Pa$^{-1}$, the die wear simulation results did not show good agreement with the worn die measurement. For this reason, some evaluation seems necessary to be done on the dimensional wear coefficient. By knowing the depth of wear from the worn die measurement and by obtaining contact pressures and sliding velocities from Finite Volume simulation of the hot forging operation, the wear coefficients have been evaluated for different points. For each section an evaluated value of the dimensional wear coefficient was obtained. These were *7.48×10$^{-13}$* , *6.75×10$^{-13}$* and *5.96×10$^{-13}$* Pa$^{-1}$, respectively. The wear profiles obtained from the evaluated wear coefficients have shown better result than the constant wear coefficient of $1\times10^{-12}\,\text{Pa}^{-1}$.

The differences of the dimensional wear coefficient in different sections are due to variation in contact pressure and sliding velocity at surface points of the die in different sections. In section 1 (see Figure 4.9), the contact pressure and the sliding velocity is relatively higher than other sections, therefore higher value of the dimensional wear coefficient is obtained.

It is obvious that at high temperatures, the hardness of die decreases. The temperature of the die surface during the hot forging operation of this study varies between 300$^{\text{o}}$C and 380$^{\text{o}}$C. The Hardness of the die material at this range of temperatures varies between 49 HRC (i.e. $H \cong 3\cdot S_y \cong 4300$ MPa, indentation hardness, $H$, is the average compression stress giving local plastic deformation on the surface) and 46 HRC (i.e. $H \cong 3\cdot S_y \cong 3750\,\text{MPa}$). By considering hardness of 4100 MPa for the die material and the

corresponding dimensional wear coefficient equal to $6.5 \times 10^{-13}$ Pa$^{-1}$, the Non-dimensional wear coefficient would be obtained as $2.66 \times 10^{-3}$.

By using the value of 4100 MPa for the hardness of the die material, and the range of 100 MPa and 300 MPa for contact pressure on the die, the normalized contact pressure (i.e. $\frac{P}{H}$) would be obtained between $2.25 \times 10^{-2}$ and $6.75 \times 10^{-2}$. During the forging operation, the sliding velocity varies between 0.1 and 0.5 m/sec. Therefore the normalized sliding velocity (i.e. $\frac{U}{a} \cdot \sqrt{\frac{A_{nom}}{\pi}}$) would obtain between 5 and 100. By comparing the evaluated value of the non-dimensional wear coefficient in this study with those suggested for mild and severe wear conditions in the wear map by Lim and Ashby [30], it can be understood that the evaluated value of wear coefficient is in the severe regime of mechanical wear. For the circumstances, the suggested wear coefficient of $3 \times 10^{-3}$ is in a good agreement with the result obtained from this thesis study.

As described in chapter 2, in a study by Porda [40], the values of dimensional wear coefficient was obtained from pin-on-disc wear test machine at room temperature as $k = (1.33 \pm 0.54) \times 10^{-13}$ Pa$^{-1}$ and $k = (2.01 \pm 1.21)$ $\times 10^{-13}$ Pa$^{-1}$, for $F_N$=21 N and $F_N$=50 N, respectively. It can be observed that the values of wear coefficients obtained in this thesis study are higher than the values given in [40]. The reasons are due to difference of temperature and the sliding velocity in hot forging operation compare to pin-on-disc wear test conditions. Therefore, higher values of wear coefficient are obtained from the hot forging experiments.

In other study, for wear analysis of warm forging dies [42], the value of non-dimensional wear coefficient obtained about $2.5 \times 10^{-4}$. The difference between the result of the thesis study and the results from [42] is due to higher contact pressure and temperature in the hot forging operation than those in the wear test. Additionally, the different materials other than the considered in the thesis study were used for dies and forging in [42].This has also effects on the results.

As sliding velocity exceeds of about 1 m/sec, the tips of asperities would be oxidized, and oxidational wear mechanism would occur [30, 33]. Since the sliding velocity is much higher than 1 m/sec on the flash land of the tested die, oxidational wear mechanism applies in this area by using Equation 2.7. For the oxidational wear mechanism a non-dimensional wear coefficient of $1.32 \times 10^{-13} \, Pa^{-1}$ was evaluated.

## 5.2 Conclusions

From the Finite Volume analysis of a closed die hot forging and wear measurement of the worn die, the following conclusions have been reached;

- Due to the sliding velocity between 0.2 and 0.5 m/sec and the contact pressure between 100 and 300 MPa on the contact interface of the die and the workpiece, the mechanical wear is predominant wear model.

- In wear analysis of dies, at the regions where high effective stresses may occur, the plastic deformation of dies must be taken into account.

- On the regions close to the parting line, due to high effective stresses plastic deformation appears. In the bottom part of the cavity, where the effective stresses are relatively lower, plastic deformation does not appear in these regions.

- Operation temperature, contact pressure, sliding velocity and contact time have great effects on the depth of wear.

- In the flash land, because of sliding velocity above 1 m/sec, the oxidational wear mechanism is observed with $k = 1.32 \times 10^{-13} \, Pa^{-1}$.

- From the simulation of hot forging process and comparison with the measurement of the worn die, the dimensional wear coefficient of $(6.5 \pm 0.6) \times 10^{-13}$ $Pa^{-1}$ (i.e. non-dimensional wear coefficient $2.66 \times 10^{-3}$) can be used as a good approximation for hot forging processes, under the same conditions.

**5.3 Future Works**

The following future studies can be suggested:

- This method can be applied for other metal forming process like warm forging or cold forging to obtain new values of wear coefficients.

- Effects of contact pressure, sliding velocity and temperature can be studied on wear coefficient.

- Simulations could also be conducted by using different simulation software packages to compare the results.

- The study can be extended for forgings with different geometries.

- A database can be prepared by study on the different die and forging materials.

- Study on relationship between the wear and coefficient of friction can be done.

# REFERENCES

[1] T. Altan, G. Ngaile and G. Shen, "Cold and Hot Forging – Fundamentals and Applications", March 2004.

[2] L. Cser, M. Geiger, K. Lange, "Tool life and tool quality in bulk metal forming", Proc. Inst. Mech. Engrs. 207 (1993) 223-239.

[3] "Metals Handbook – Forging and Casting", Vol. 5, 8th Edition, ASM Handbook Committee, USA, 1971.

[4] T. Altan, F. W. Boulger, J. R. Becker, N. Akgerman, H. J. Henning, "Forging Equipment, Materials and Practices", Batelle Columbus Laboratories Metalworking Division, Ohio, 1973.

[5] J, R. Sabroff, F.W. Boulger, H. J. Henning, "Forging Materials and Practices", Batelle Memorial Institute Columbus, Ohio, 1968.

[6] T. Altan, H. J. Henning, "Closed-Die Forging of Round Shapes – Flash Design and Material Savings", Metallurgia and Metalforming, March, p. 83, 1972.

[7] M. Terčelj, I. Peruš, R. Turk, "Suitability of CAE Networks and FEM for Prediction of Wear on Die Radii in Hot Forging", Tribology International, 36, 2003, 573-583.

[8] Private Communications with AKSAN Steel Forging Company.

[9] Uddeholm Tool Steel, www.ramada.pt/acos/pdf/pdf/Dievar.pdf

[10] J.H. Kang, I.W. Park, J.S. Jae, S.S. Kang, "A study on a die wear model considering thermal softening (I): construction of the wear model", J. Mater. Process. Technol. 96 (1999) 53–58.

[11] R. Douglas, D. Kuhlmann, "Guidelines for Precision Hot Forging with Application", Journal of Material Processing Technology, pp. 182-188, 2000.

[12] A.N. Bruchanow, A. W. Rebelski, "Gesenkschmieden und Warmpressen", Verlag Technik, Berlin, 1955.

[13] A. Bramley; Forging Modelling. Proc. of the 9th Intern. Cold Forging Congress, pp 165-168, 1995.

[14] W. J. Slagter, C. J. L. Florie and A. C. J. Venis, "Advances in 3-D Forging Process Modeling", MSC.Software Corporation, Groningenweg 6, 2803 PV Gouda, The Netherlands.

[15] P. Ding, D. Ju, T. Inoue, E. Vries, "Numerical Simulation of Forging and Subsequent Heat Treatment of a Rod by a Finite Volume Method", ACTA Metallurgica Sinica (English Letters), Vol. 13, No. 1, pp 270-280, February, 2000.

[16] A. E. Tekkaya, "Current State and Future Developments in the Simulation of Forming Processes". Proc. 30th Plenary Meeting of the International Cold Forging Croup ICFG, Den Bosch, September1997, pp.1-10.

[17] W. J. Slagter, C. J. L. Florie and A. C. J. Venis, "Forging Simulation Tool Based on Breakthrough Technology", MSC.Software Corporation, The Netherlands.

[18] V. Bhavin Mehta, Ibrahim Al-Zkeri, Jay S. Gunasekera, "Evaluation of MSC.SuperForge for 3D Simulation of Streamlined and Shear Extrusion Dies", Ohio University, Athens, Ohio, USA, 2000.

[19] MSC.SuperForge 2004, User Guide.

[20] M. Ceran, "Finite Element Analysis of Cold Upset Forging Dies", M. Sc. Thesis, Middle East Technical University, Ankara, Turkey, 2002.

[21] D. Elmaskaya, "Finite Element Analysis of Effects of Tapered Preforms in Cold Upsetting", M. Sc. Thesis, Middle East Technical University, Ankara, Turkey, 1997.

[22] S. Isbir, "Finite Element Analysis of Trimming Process", M. Sc. Thesis, Middle East Technical University, Ankara, Turkey, 2002.

[23] Ö. Dogan, "Finite Element Analysis of Effects of Tapered Preforms on Final Product in Cold Upsetting", M. Sc. Thesis, Middle East Technical University, Ankara, Turkey, 2000.

[24] E. Alper, "Computer Aided Design of Axi-Symmetric Press Forgings", M. Sc. Thesis, Middle East Technical University, Ankara, Turkey, 1989.

[25] A. E. Kutlu, "Analysis and Design of Preforms for Non-Axisymmetric Press", M. Sc. Thesis, Middle East Technical University, Ankara, Turkey, 2001.

[26] A. B. Karagözler, "Analysis and Preform Design for Long Press Forgings with Non-Planar Parting Surfaces", M. Sc. Thesis, Middle East Technical University, Ankara, Turkey, 2003.

[27] S. Gülbahar, "Preform Design for Forging of Heavy Vehicle Steering Joint", M. Sc. Thesis, Middle East Technical University, Ankara, Turkey, 2004.

[28] B. Civelekoğlu, "Analysis of Forging for Three Different Alloy Steels", M. Sc. Thesis, Middle East Technical University, Ankara, Turkey, 2003.

[29] J.A. Williams, Engineering Tribology, Oxford University Press, ISBN 0 19 856503 8, 1998.

[30] S. C. Lim, M. F. Ashby, "Wear mechanism maps", Acta Metallurgica, 35(1), 1-24, 1987.

[31] J.F. Archard, W. Hirst, "The wear of metals under unlubricated conditions", Proc. R. Soc., Ser A 236 1956 397–410.

[32] K. Nakajima and Y. Mizutani, "structural change of the surface layer of low carbon steels due to abrading", Wear 13, 283, 1969.

[33] T. F. J. Quinn, J.L. Sullivan and D. M. Rowson, "Origins and development of oxidational wear at low ambient temperature", Wear 94, 175, 1984.

[34] J.F. Archard, "Contact and rubbing of flat surfaces", J. Appl. Phys. 24 981, 1953.

[35] M. M. Kruschov, "Resistance of metals to wear by abrasion, as related to hardness", Proc.   of Conf. on Lub. and Wear. Inst. of  Mech. Engrs, London, PP. 655-59, 1957.

[36] J.A. Williams, "Wear modeling: analytical, computational and mapping: a continuum mechanical approach", Wear 225-229, 1-17, 1999.

[37]T. Sobis, U. Engel, M. Geiger, "A theoretical study on wear simulation in metal forming process", J. Mater. Process. Technol. 34, 233–240, 1992.

[38] B. Painter, R. Shivpuri, T. Altan, "Prediction of die wear during hot-extrusion of engine valves", J. Mater. Process. Technol. 59, 132–143, 1996.

[39] G.A. Lee, Y.T. Im, "Finite-element investigation of the wear and elastic deformation of dies in metal forming", J. Mater. Process. Technol. 89–90 123–127, 1999.

[40] P. Porda, S. Anderson, "Simulating sliding wear with finite element method", Tribology international 32, 71-81, 1999.

[41] J.H. Kang, I.W. Park, J.S. Jae, S.S. Kang, "A study on a die wear model considering thermal softening (II): application of the suggested wear model", J. Mater. Process. Technol. 94 (1999) 183–188.

[42] R. S. Lee, J. L. Jou, "Application of numerical simulation for wear analysis of warm forging die", J. Mater. Process. Technol. 140, 43-48, 2003.

[43] Pro/Engineer User Guide, PTC, Release 2001.

[44] MSC. Marc 2001, User Guide.

[45] MSC.SuperForge, Material Library.

[46] MSC.Superforge User Guide, the MacNeal-Scwendler Corporation, Release 2002.

[47] MSC.SuperForge 2004, User Guide, Sample simulation of closed die forging with flash.

[48] By selecting DIEWEAR option in MSC.SuperForge, this value is available at RUN file in the current PROCESS Directory of simulation.

[49] Reference Manual of PC-DMIS™ 3.6, 2002-2003 Brown & Sharpe Manufacturing Corporation and Wilcox Associates Incorporated.

[50] www.matweb.com, Online Material Property Data Sheet, October 2004.

# APPENDIX A

## METHOD OF SURFACE MEASUREMENT
## BY USING CMM

The first step in CMM part programming is to define which probes will be used during the inspection process. PC-DMIS supports a wide variety of probe types, for this measurement the extension of 200 mm length and tip with 1 mm diameter are selected that are shown in Fig. 3.2. After this step the surface measurement can be done by selecting PATCH method and defining needed parameters. In this method four boundary points should be define to form the edges of surface limits which is going to be measured. Patch method



Fig. A.1 PC-DMIS Used in
METU-BILTIR Center



Fig. A.2 Extension of 200mm length
and tip with 1mm diameter.

will scan the surface depending on the selected techniques (Line, Body Axis or Variable) for Direction 1 Tech area and Direction 2 Tech. The probe will always remain within the cut plane while doing the scan. The Direction 1 technique indicates the direction between the first and second boundary points.

The Direction 2 technique indicates the direction between the second and third boundary points. PC-DMIS will scan the part on the surface indicated by the Direction 1 Tech area. When it encounters the second boundary point, PC-DMIS will automatically move to the next row as indicated by the Direction 2 Tech area. The Patch scans, as shown in Fig. 3.3. is like a series scans done parallel to each other [49].
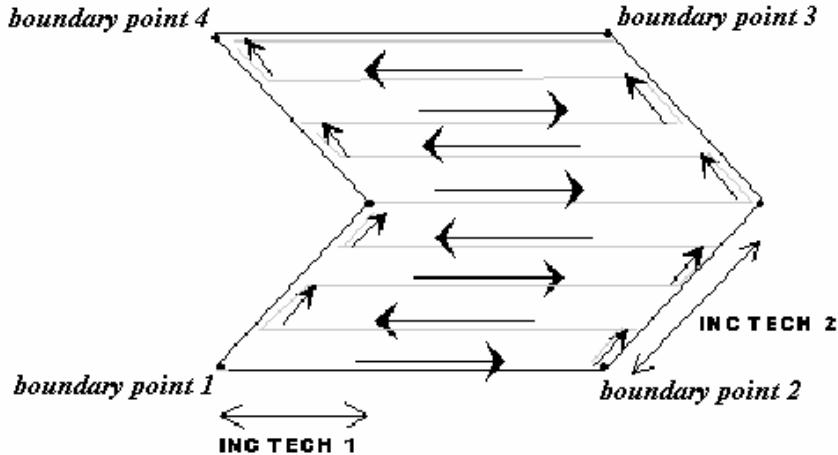


Fig. A.3 PATCH method scans for surface measurement [45].

Three different techniques are available for PATCH scan, for this measurement the most accurate method is selected which is VARIABLE method. The VARIABLE technique allows you to set specific maximum and minimum angle and increment values that will be used in determining where PC-DMIS will take a hit. The probe's approach is perpendicular to the line between the last two measured hits. The technique is shown in Fig. 3.4. The maximum and minimum values that will be used to determine the increments between hits must be entered; also the desired values for the maximum and minimum angles must be entered. PC-DMIS will take three hits using the minimum increment. It will then measure the angle between hit's 1-2 and 2-3.
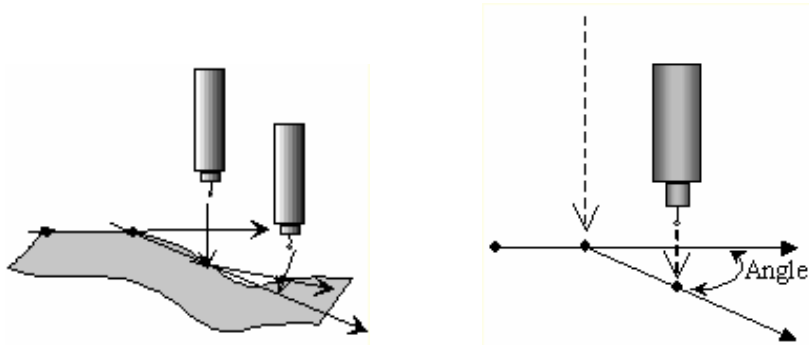
Fig. A.4 The VARIABLE technique for surface measurement.

- If the measured angle is between the maximum and minimum values defined, PC-DMIS will continue to take hits at the current increment.

- If the angle is greater than the maximum value, PC-DMIS will erase the last hit and measure it again using one quarter of the current increment value.

- If the angle is less than the minimum increment, PC-DMIS will take the hit at the minimum increment value.

PC-DMIS will again measure the angle between the newest hit and the two previous hits. It will continue to erase the last hit and drop the increment value to one quarter of the increment until the measured angle is within the range defined, or the minimum value of the increment is reached.

- If the measured angle is less than the minimum angle, PC-DMIS will double the increment for the next hit.

- If this is greater than the maximum increment value it will take the hit at the maximum increment.

PC-DMIS will again measure the angle between the newest hit and the two previous hits. It will continue to double the increment value until the measured angle is within the range defined, or the maximum increment is reached.

The Max increment and Min increment allow setting the maximum and minimum increment distances. Even though increments may increase than maximum value or decrease than minimum value while using the Variable option, the increment will never is greater than maximum value and less than minimum value.

The Max angle and Min angle allow setting the maximum and minimum angles. Even though angles measured may increase or decrease while using the Variable option, the angle will never is greater than maximum value and less than minimum value.

The last step is defining Move speed and Touch speed of probe; these will be defined as percentage of maximum speed of the probe.

# APPENDIX B

## MATERIAL PROPERTIES

**Material Properties of Steel DIN 1.4021**

**Subcategory:** Heat Resisting; Stainless Steel; T 400 Series Stainless Steel [50].

**Close Analog:** X20Cr13, AISI Type 420 Stainless Steel.

**Composition (%):**

| C | Cr | Fe | Mn | P | S | Si |
|---|---|---|---|---|---|---|
| Min 0.15 | 13 | 85 | Max 1 | Max 0.04 | Max 0.03 | Max 1 |

**Physical Properties:**

Density        : 7.87 g/cm$^3$

Hardness       : 195 HBr, 12 HRc-C (annealed bar at room temperature)

**Mechanical Properties (at room temperature):**

Tensile Strength (Ultimate) : 655 MPa

Tensile Strength (Yield) : 345 MPa

Bulk Modulus : 140 GPa

Shear Modulus : 80.7 GPa

Poisson's Ratio : 0.24
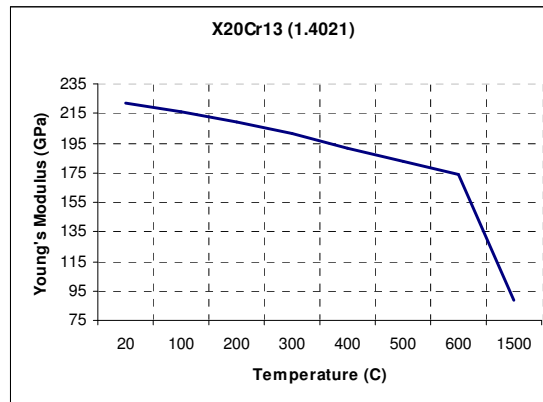


Fig. B.1 Young's Modulus of X20Cr13 function of temperature [45].

**Thermal Properties :**
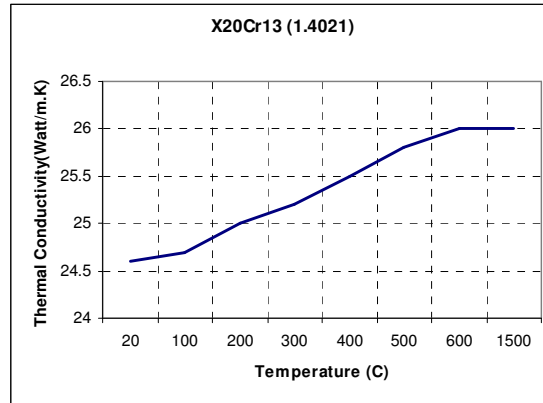


Fig. B.2 Thermal conductivity of X20Cr13 function of temperature [45].
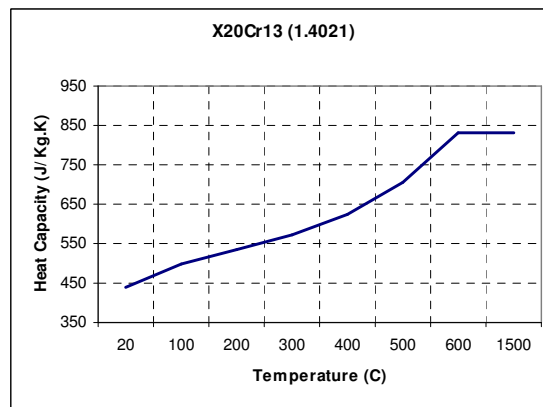


Fig. B.3 Heat capacity of X20Cr13 function of temperature [45].
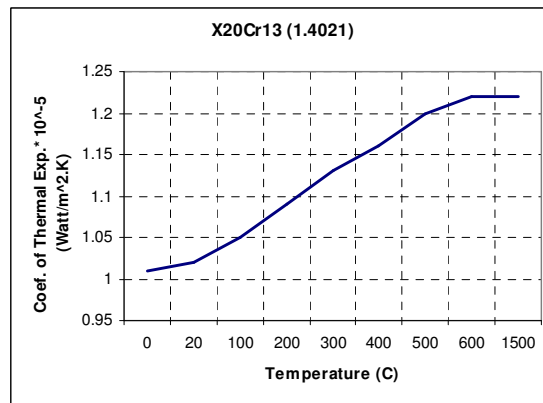


Fig. B.4 Coefficient of thermal expansion of X20Cr13 as a function of temperature [45].

**Material Properties of Alloy Tool Steel AISI L6**

**Subcategory:** Oil-Hardening Steel; Tool Steel [50].

**Close Analog:** 55NiCrMoV7, DIN 1.2714.

**Composition (%):**

| C | Cr | Fe | Mn | Ni | Si | V |
|------|------|-------|------|------|------|-----|
| 0.7 | 1 | 95.95 | 0.35 | 1.75 | 0.25 | 0.1 |

**Physical Properties:**

Density         : 7.86 g/cm$^3$

Hardness         : 45 HRc-C

**Mechanical Properties (at room temperature):**

Young's Modulus: 200 GPa

Poisson's Ratio: 0.3

Shear Modulus : 80 GPa

**Thermal Properties :**

Thermal Conductivity: 46 watt/ m.K

Specify Heat & Heat Capacity:  420 J/ Kg.K

Coefficient of Thermal Expansion: $1.5 \times 10^{-5}$
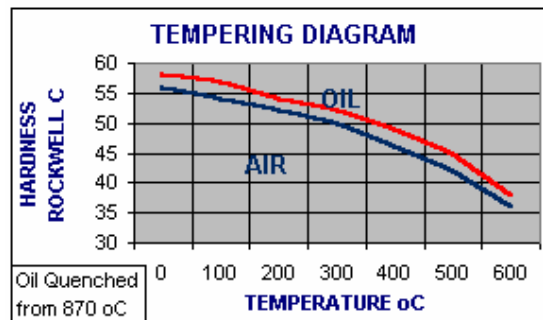


Fig. B.5 Tempering diagram of AISI L6 tool steel [50].